ADVANCED FUNCTIONAL MATERIALS
www.afm-journal.de

Bioinspired Artificial Eyes: Optic Components, Digital Cameras, and Visual Prostheses

Gil Ju Lee, Changsoon Choi, Dae-Hyeong Kim, and Young Min Song**

The diverse vision systems found in nature can provide interesting design inspiration for imaging devices, ranging from optical subcomponents to digital cameras and visual prostheses, with more desirable optical characteristics compared to conventional imagers. The advantages of natural vision systems include high visual acuity, wide field of view, wavelength-free imaging, improved aberration correction and depth of field, and high motion sensitivity. Recent advances in soft materials, ultrathin electronics, and deformable optoelectronics have facilitated the realization of novel processes and device designs that mimic biological vision systems. This review highlights recent progress and continued efforts in the research and development of bioinspired artificial eyes. At first, the configuration of two representative eyes found in nature: a single-chambered eye and a compound eye, is explained. Then, advances in bioinspired optic components and image sensors are discussed in terms of materials, optical/mechanical designs, and integration schemes. Subsequently, novel visual prostheses as representative application examples of bioinspired artificial eyes are described.

1. Introduction

Humanity has devoted significant effort over a long time to the development of imaging devices capable of detecting and/or recording moving objects as humans see them. Camera-related technologies have matured continuously, imitating key factors of the human eye, such as the lens and retina, using artificial optical lenses and electronic devices. The current level of digital camera technology has reached and surpassed the capabilities of biological eyes (e.g., human eyes) in terms of resolution and perception mechanisms.[1–3] However, regarding simplicity, miniaturization, energy efficiency, and certain functional aspects, conventional imaging technologies still have significant room for improvement compared to animal's eyes.[4,5] For instance, common digital cameras require complicated lens configurations due to the mismatch between the imaging surface and the focal plane (i.e., the Petzval surface), whereas the natural eyeball only has a single lens. Extremely compact cameras with such designs are of interest in both smartphone and drone applications and in robot eyes and visual prostheses. Efficient light management in the natural eye, such as light accommodation or adaptation, is also an important natural facet that should be mimicked in artificial eye research.[6–11]

The diversity of light sensing organs in nature drives the development of novel camera systems that adopt unconventional geometry and functions to provide superb performance beyond existing technologies. In contrast to the human eye (i.e., a single-chambered eye), compound eyes as can be found in insects, crustaceans, and other arthropods are particularly remarkable for their extremely wide field of view (FoV), nearly infinite depth of field, and high motion sensitivity.[12,13] The potential applications of compound eye-inspired technology include navigation and sensing devices, biomedical endoscopies, and security cameras. Optical subcomponents in compound eyes such as microlens arrays (MLAs) in the cornea, antireflective nanostructures, and reflection/refraction-type waveguiding units are of great importance in the field of bioinspired photonics.[14–18]

Another important stream of bioinspired image sensor research is medical applications such as the visual prostheses.[19,20] Human eye-inspired optoelectronic systems can restore the vision of patients with retinal degeneration.[21] Visual prostheses are designed to mimic the human retina, providing light detection and neural signal generation. Such prostheses act as an intact retina in the patient's eye. However, the basic architecture of visual prostheses to date requires further breakthroughs in several aspects, such as visual acuity,[22,23] FoV,[24,25] and lifetime.[26,27] These technological advances are hindered by material and device design limitations, such as low pixel density, small area coverage of the prosthetic device, material biocompatibility, and inflammation associated with long-term implantation.[28–30] Such circumstances demand retina-like electronics that are extremely soft and thin, sensitive to light, apply stimulation precisely to a tiny spot, and achieve large-area coverage, thus facilitating the enhanced functionality and long-term biocompatibility of the visual prosthesis.[26,28]

The past decade has seen enormous progress in the development of bioinspired artificial eyes due to huge engineering efforts

G. J. Lee, Prof. Y. M. Song
School of Electrical Engineering and Computer Science (EECS)
Gwangju Institute of Science and Technology (GIST)
Gwangju 61005, Republic of Korea
E-mail: ymsong@gist.ac.kr
C. Choi, Prof. D.-H. Kim
Center for Nanoparticle Research
Institute for Basic Science (IBS)
Seoul 08826, Republic of Korea
E-mail: dkim98@snu.ac.kr
C. Choi, Prof. D.-H. Kim
School of Chemical and Biological Engineering
Institute of Chemical Processes
Seoul National University
Seoul 08826, Republic of Korea

DOI: 10.1002/adfm.201705202

that have bridged the gap between conventional technologies that rely on rigid materials and planar designs and biological eyes based on soft tissues and curved shapes.[31–42] Recently developed flexible and stretchable electronics technologies combined with soft materials and devices[43,44] have facilitated the development of a new class of imaging systems and visual prostheses.[26,45,46] Here, we review recent advances in bioinspired artificial eyes with an emphasis on approaches based on soft materials/structures, and their integration technology toward outstanding optical systems and visual prostheses. The article starts by presenting descriptions of the representative eyes being actively researched (i.e., single-chambered eyes and compound eyes). The subsequent sections discuss schemes for implementing bioinspired graded index lenses, soft light-management components similar to biological eyes, curved photodetector arrays, 3D/micro-optical components/systems, compound eye cameras, and advanced visual prostheses, in each case with representative examples that describe their functionalities and remaining challenges. Finally, a short perspective concludes the review.

2. Eye Evolution and High-Resolution Vision

The evolution of the eye was driven by the demand for the capability to process more complex sensory tasks. As the amount of information increases, the necessary information-processing capacity gradually becomes more complex, thereby necessitating more sophisticated sensory organs (**Figure 1**a).[47] For example, a nondirectional photoreceptor is appropriate for animals that only require the simple monitoring of the ambient light intensity of the external environment, such as measuring the water depth, indicating the level of ultraviolet radiation, or detecting shadows. Animals that employ phototaxis exploit a directional photoreceptor to determine the light's direction. Such low-resolution vision systems consist of an array of directional photoreceptors, such as pit or cup eyes found in nautiluses. While these exhibit crude low resolution, such eyes serves as a very efficient sensory system to obtain the flow field for self-motion that controls the speed and direction of locomotion. More complicated tasks such as the detection of prey or predators, visual communication, and mate recognition have led to high-resolution vision. Thereby, evolution to the most efficient sensory organs matching with the inhabited environment has yielded these four classes of eyes.

High-resolution vision eyes such as the human eye (Figure 1b) and apposition compound eye (Figure 1c) are representatives of single-chambered eyes and compound eyes, which are typically found in vertebrates/chelicerates and insects/crustaceans, respectively, have triggered a recent renaissance in bioinspired imaging systems.[45–53] The human eye has a simple configuration (i.e., the eyeball) composed of a single lens, a concavely hemispherical retina, and light-management components for accommodation and adaptation, as illustrated in Figure 1b. Meanwhile, the apposition compound eye is mainly composed of several ommatidia on a convex hemisphere. An ommatidium is a unit optical channel that uses micro-optics to focus light and rhabdoms that convert light into neural signals, as shown in Figure 1c.

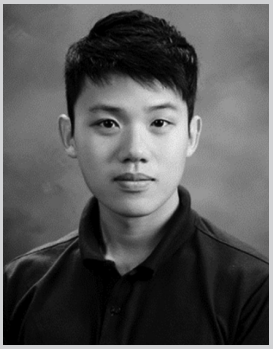

Gil Ju Lee received his B.S. (2016) from the Department of Electronics Engineering at the Pusan National University and is a Ph.D. candidate under the guidance of Prof. Young Min Song in the Gwangju Institute of Science and Technology (GIST). His current research interests focus on bioinspired imaging systems and biophotonic structures.

Changsoon Choi received his B.S. (2012) from the Department of Material Science and Engineering at the Seoul National University and his M.S. (2014) from the School of Chemical and Biological Engineering at the Seoul National University. Under the supervision of Prof. Dae-Hyeong Kim, he is working on the fabrication of human-eye-inspired imaging systems.

Dae-Hyeong Kim received his B.S. (2000) and M.S. (2002) degrees from the School of Chemical Engineering at the Seoul National University. He obtained his Ph.D. (2009) from the Department of Materials Science and Engineering at the University of Illinois at Urbana–Champaign. Since he joined the faculty of the School of Chemical and Biological Engineering at the Seoul National University in 2011, he has focused on stretchable electronics for biomedical and bioinspired imaging applications.

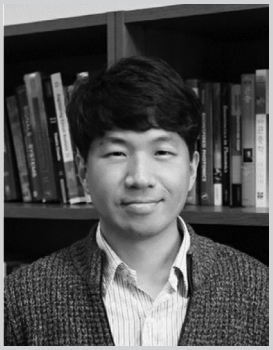

Young Min Song received a M.S. and Ph.D. in Information and Communications from the Gwangju Institute of Science and Technology (GIST) in 2006 and 2011, respectively, after a B.S. degree in Biomedical Engineering from the Yonsei University in 2004. From 2011 to 2013, he was a postdoctoral research associate in the Department of Materials Science and Engineering at the University of Illinois at Urbana–Champaign. He is currently an assistant professor in the School of Electrical Engineering and Computer Science at the GIST. His research includes multifunctional nanophotonics, advanced optoelectronic devices/systems, and optical healthcare systems.

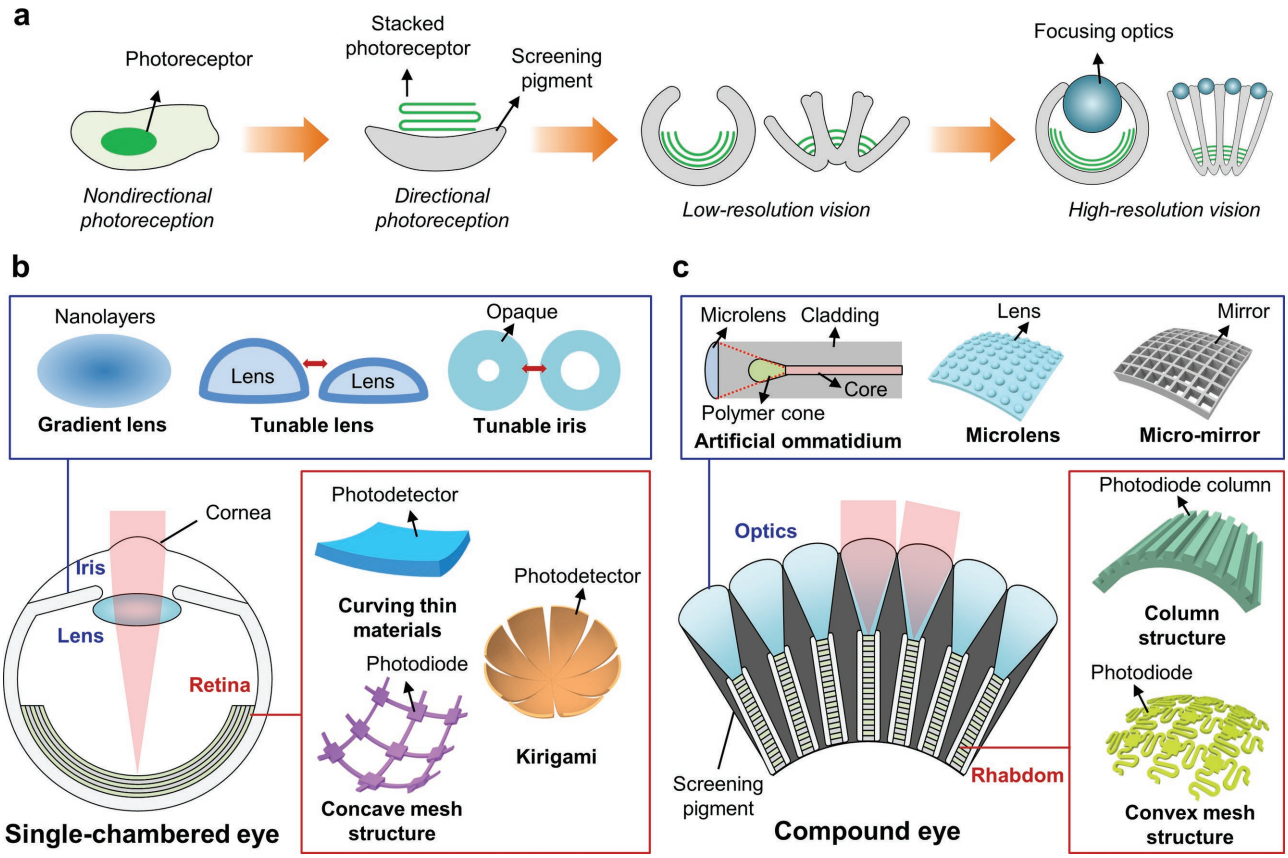

Figure 1. a) Evolution of eyes from nondirectional photoreceptors to high-resolution vision corresponding to single-chambered eyes (left) and compound eyes (right). Schematic illustrations of the major components of bioinspired imaging systems: b) single-chambered eyes and c) compound eyes.

The remarkable imaging features of the human eye (i.e., wide FoV of up to 95°, high resolution of 1 arcmin per line pair at the fovea, active accommodation/adaptation to the light environment, and simple configuration)[1] originate from the unusual refractive index distribution that reduces aberrations in the crystalline lens,[54] a focal length tunability by the crystalline lens and ciliary body,[1] and the hemispherical retina that facilitates a wide FoV and low aberrations.[55] In contrast to the human eye, the absence of materials and techniques to assemble a graded refractive index (GRIN) lens, focal length-tunable lens, and curvilinear image sensors forces the selection of a multilens configuration and electrical/mechanical/optical subsystems as strategies of modern optics.[56–58]

A sophisticatedly formed apposition compound eye can simultaneously capture several objects in a wide FoV without a head movement due to its hemispherical shape and the individual imaging of each ommatidium, which is a single imaging unit. Individual imaging, which is enabled by micro-optics and rhabdoms, offers at least three advantages: a nearly infinite depth of field, high motion sensitivity, and the absence of geometrical distortion and aberrations.[4,12] These imaging characteristics are also found in other anatomies of compound eyes. In contrast to the apposition type observed in diurnal insects, different classes of compound eye such as refracting/reflecting/parabolic and neural superposition types can be found in nocturnal insects and crustaceans living in water and exhibit exceptional imaging properties in weak ambient light.[59]

Recent applications including smartphones, autonomous vehicles, navigation, surveillance, and biomedicine drive a need for smaller and simpler imaging devices with the appealing optical features found in biological eyes (i.e., high resolution, wide FoV, high motion sensitivity, low aberrations, etc.), thus highlighting the necessity of research into bioinspired imaging devices. Recent advances in bioinspired imaging systems have led to material and structural schemes that mimic the light-management components and curved retina or rhabdoms of the single-chambered eye and the compound eye. Figure 1b,c shows representative examples in red and blue boxes. The following sections introduce the specific classes and principles of recently developed bioinspired optical elements, and the key challenges for addressing the current issues of biomimetics in imaging devices.

3. Biomimicry of Single-Chambered Eyes

In nature, many animals including both vertebrates and invertebrates, such as octopuses, squids, and spiders, have single-chambered eyes.[4] Depending on their habitat, lens shapes are classified as either spherical or aspherical, because the lenses' desired focusing power differs.[54] Animals' position in the food

chain also affects the features of their eyes.[60] For instance, the eyes of predators are placed frontally to provide wide binocular fields and have a fovea capturing objects at high resolution. The two images captured by the eyes present slightly different perspectives, and hence offer depth information. In contrast, animals considered as prey possess laterally directed eyes and very little binocular overlap. Rabbits and rats do not have a fovea, but rather a horizontal "visual streak" with an increased density of ganglion cells that image the horizon environment to search for food, predators, and relatives.[60]

Although single-chambered eyes have a broad distinction according to habitat and food chain, a single lens and hemispherical retina are commonalities in all single-chambered eyes. Therefore, implementing a high-performance single lens and hemispherical retina are key points in the biomimicry of single-chambered eyes. Aside from these two components, other light management components can be mimicked, such as the ciliary body changing the focal length (i.e., accommodation) and an iris to control the amount of incoming light (i.e., adaptation). Thus, subsections in this chapter discuss the specific working principles of mimicked optical subcomponents (i.e., lens, accommodation, and adaptation). Subsequently, approaches to the implementation of the curved retina are also described and representative examples given.

3.1. Artificial Optical Apparatus Mimicking Biological Eyes

Human eyes possess an aspherical crystalline lens with a GRIN distribution to correct optical aberrations (**Figure 2**a).[61] Unfortunately, materials with GRIN capabilities are scarce among glasses and polymers that can be exploited as optical lenses. Therefore, modern optics employ the option of using multiple lenses with different optical dispersions to compensate for aberrations, but this typically demands heavy and large optical designs. Hence, the fabrication technology of aspherical GRIN

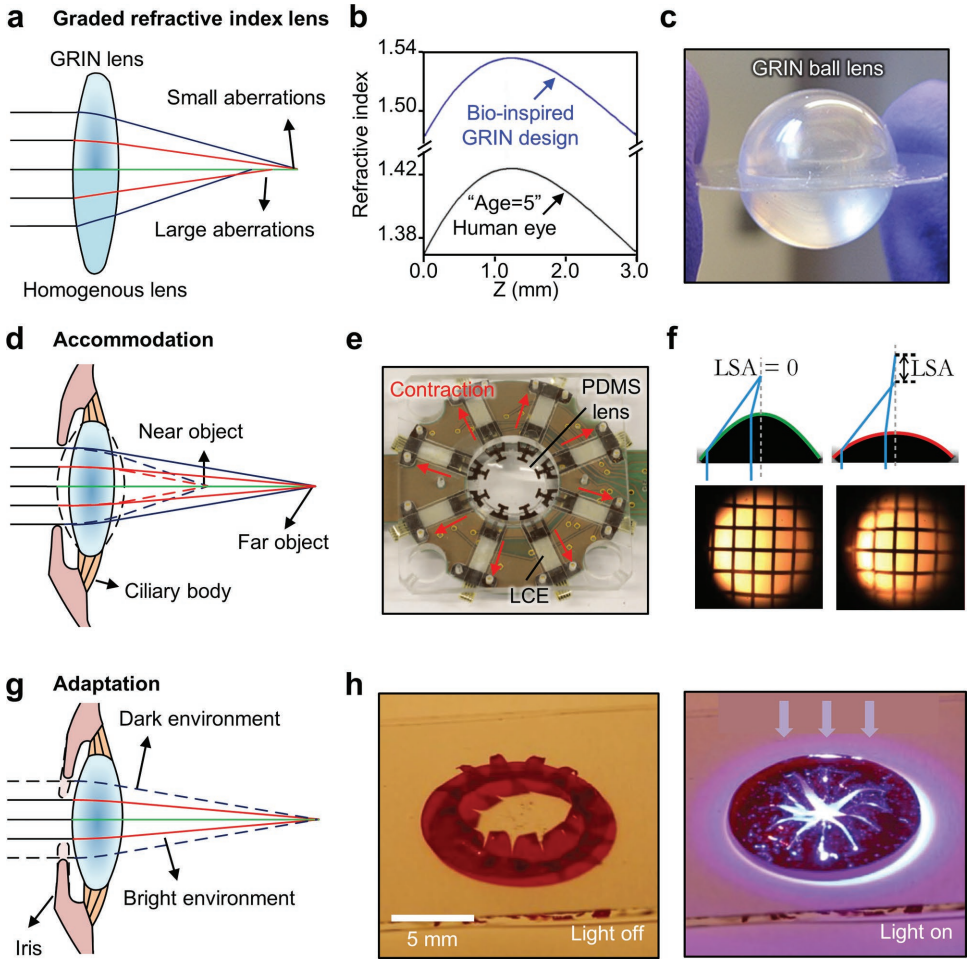

Figure 2. Optical components inspired by single-chambered eyes. a) Ray tracings for homogeneous lens and graded refractive index (GRIN) lens. b) Refractive index profile of a GRIN lens mimicking a human eye. Reproduced with permission.[54] Copyright 2012, The Optical Society. c) Image of a GRIN ball lens. Reproduced with permission.[62] Copyright 2013, SPIE. d) Schematic illustration of the accommodation in a single-chambered eye. e) A deformable liquid crystal elastomer (LCE)-actuated PDMS-based lens. Reproduced with permission.[64] Copyright 2016, Nature Publishing Group. f) Cross-sectional views of a fluidically tunable lens with an aspherical surface for correcting longitudinal spherical aberration. Reproduced with permission.[66] Copyright 2014, Nature Publishing Group. g) Schematic illustration of adaptation in a single-chambered eye. h) Photographs of an artificial iris: wide (left) and narrow (right) states. Reproduced with permission.[75] Copyright 2017, WILEY-VCH.

lenses can offer many advantages to modern optics, including simplicity of optical systems and low incidence of optical aberrations. One strategy for mimicking the GRIN lens in the human eye is synthesizing polymers by utilizing a nanolayered polymer film-based technique.[54] The lens fabrication process has three steps: First, create GRIN anterior and posterior lenses using a coextruded poly(methyl methacrylate) (PMMA)/SAN17 nanolayered optical film whose gradual refractive index is in the range 1.489–1.573. The synthesized polymeric GRIN lens is then carved and polished by diamond turning. Finally, the human eye-inspired GRIN lens is formed by merging the anterior and posterior GRIN lenses; related refractive index profiles are shown in Figure 2b.[54]

The spherical GRIN lens that can be found in many aqueous animals exhibits more appealing optical features due to its shape compared to land creatures, including the elimination of most aberrations and the capability to capture panoramic views. One path to implementing a spherical GRIN lens involves forming a series of nested spherical shells that can adhere together to form a spherical lens. The spherical shells possess a graded refractive index that can be realized with the technique utilized when mimicking the human eye (Figure 2c).[62] Another fabrication route for GRIN lenses is using recently emerging metamaterials.[63] Although metamaterial-based GRIN lenses do not cover the wavelength range in which we are interested (i.e., visible or near infrared), it presents the possibility that metamaterials could be used to mimic biological lenses.

In human eyes, accommodation, which refers to adjusting the focal length by changing the shape of the crystalline lens with the support of the ciliary body that acts as a contractor muscle, is vital for obtaining a clear image of objects at different distances (Figure 2d). Mimicking accommodation involves two strategies: (1) using a plastic ciliary body and elastomeric lens, and (2) fabricating a shape-changeable lens that responds to physical actuation. The first strategy exploits a liquid crystal elastomer (LCE) that can be used as an artificial ciliary body to control the shape of an elastomeric lens (Figure 2e).[64] The LCE is a mixture of elastomer and liquid crystal with the ordering properties of a liquid crystal. The ordering property of the liquid crystal provides two phases (e.g., ordered and disordered states) to the LCE. A phase transition induced by temperature variation significantly changes the LCE's length, deforming the elastomeric lens' shape. The use of a shape-changeable lens is usually based on a liquid-injectable lens where the injected liquid deforms the curvature of the lens and thus varies its focal length.[49,65] Recently introduced liquid-based lenses with the support of electric fields also facilitate the reduction in longitudinal spherical aberrations by easily shaping aspherical lenses (Figure 2f),[66] which is a challenging task in rigid optics. Other physical actuation methods include electrically shape-tunable lens systems[67–70] and mechanics-based accommodation.[70]

Excessively strong light can damage the retina and weak light hinders object recognition; the human eye has an iris to adapt to light environment variation (Figure 2g). Many schemes with various actuation mechanisms have sought to mimic this form of adaptation, such as electromagnetic heating,[71] electrowetting in microfluidics,[72,73] and piezomechanics;[74] however, such schemes require separate external controllers. A recently introduced approach based on a novel material that directly reacts to light provides an active accommodation device that can eliminate the need for an external control unit. The device exploits the concepts of the anisotropic thermal expansion of LCE and the radial alignment of all LCE segments. The thermal energy induced by light radiation creates stress and thus bends LCE segments in the opposite direction to the initial bending state, i.e., a closed state (Figure 2h).[75]

The diversity of material design and synthesis methods paves the way for the materialization of exceptional optical lenses and adjustable soft optics with light-control capabilities, which is not observed in rigid material-based modern optics. By introducing other intriguing single-chambered eyes, permits the realization of extraordinary properties (e.g., a wide FoV/removal of most aberrations,[76,77] strong light absorption structures for scotopic vision,[78] and hyperacuity[79]).

3.2. Retina-Inspired Curved Photodetector Arrays

The arch shape of the retina in most single-chambered eyes offers inspiration for reducing optical systems' complexity. The light from the external environments forms focal spots along the curved shape (i.e., the Petzval surface).[55] Current image sensor technologies based on charge-coupled device (CCD) and complementary metal-oxide semiconductor (CMOS) architectures provide excellent capabilities such as high speed, low cost, low power consumption, and superb photon capturing, but cannot offer a path to the development of curvilinear image sensors that correspond to the retina. As with the correction of optical aberrations, flattening the optimum focal plane of an optical design requires a multilens configuration, which is complex, large, and heavy. Meanwhile, the use of a curved image sensor facilitates a simple optical configuration by matching the image sensor with the focal plane.[55,57,80,81]

Curving thinly ground CMOS/CCD image sensors serves as a strategy for mimicking the retina's curvilinear shape. Conventional cameras usually consist of a thick single-crystalline Si photodetector array that hinders the curving of image sensors due to its high stiffness, low fracture roughness, and high modulus (2–5 GPa).[82] However, thin Si (25 μm) can provide low strain for a curved imager, and hence can be curved to a radius of less than 1 mm without fracturing.[82] In this scheme, the curved image sensor based on a bulk CMOS/CCD image sensor is formed by thinning, placing the thinly ground image sensor into a mold, and deforming via pneumatic pressure (**Figure 3**a). Figure 3b highlights a successful example with a ≈19 mm radius of curvature (RoC), which is the highest curvature attained in a curved image sensor to date based on this scheme.[82] However, bulk curved image sensors still demand further improvements in coverage area and RoC compared to single-chambered eye systems. For example, the human eye's retina covers most of the hemispherical chamber, and the RoC of the human eye is as small as 12 mm.[1]

Other strategies use intrinsically soft materials (for example, organic,[83–85] 0D/1D/2D nanomaterials,[86–89] and perovskites[90–92]) or additional optical subsystems to capture images on a curved focal plane.[93] Inherently soft materials provide high bendability and thus facilitate the fabrication of highly curved photodetector arrays (Figure 3c).[87] However,

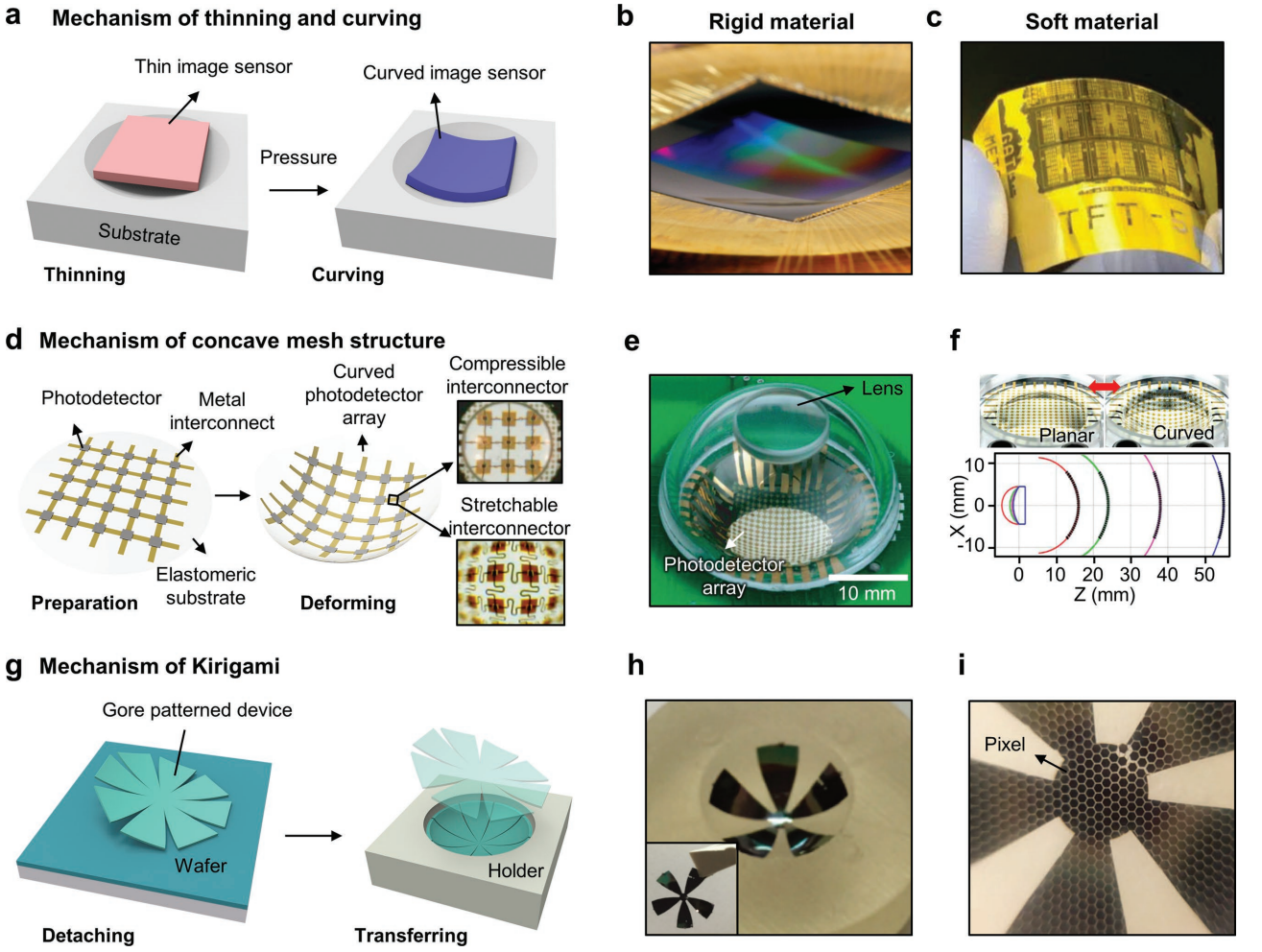

Figure 3. Retina-inspired curved image sensors. a) Schematic illustration of the curving deformation method for an inorganic image sensor. b,c) Images of representative examples: (b) Rigid material-based. Reproduced with permission.[82] Copyright 2017, The Optical Society. (c) Soft material-based. Reproduced with permission.[87] Copyright 2015, WILEY-VCH. d) Schematic illustration of a concave mesh structure. The interconnector that allows 3D deformation between each pixel is classified as either compressible (Reproduced with permission.[46] Copyright 2008, Nature Publishing Group.) or stretchable. (Reproduced with permission.[49] Copyright 2011, National Academy of Sciences.) e) Representative image of a simple imaging system inspired by the human eye based on a concave mesh structure. Reproduced with permission.[46] Copyright 2008, Nature Publishing Group. f) Tunable photodetector array based on a stretchable interconnector that facilitates matching the optimum curvature of the image plane, which can vary depending on the lens curvature. Reproduced with permission.[49] Copyright 2011, National Academy of Sciences. g) Schematic illustration of a kirigami-based curved photodetector array fabrication method. h) Image of a hemispherical photodetector array based on the kirigami technique. The inset shows the device detached from the substrate. Reproduced with permission.[97] Copyright 2016, Nature Publishing Group. i) Magnified view of the kirigami-based device's high pixel density. Reproduced with permission.[97] Copyright 2016, Nature Publishing Group.

hemispherical deformation of planar photodetector arrays with flexibility is difficult because additional stretchability is required in 3D deformation. A fiber-shaped photodetector[94] that facilitates omnidirectional photon capturing has been reported to address this, but it has limitations such as detection wavelength (i.e., UV range). Optical fiber bundle arrays located along a curved surface are introduced as an exclusively different approach; this has the same effect as a curved image sensor but using a flat image sensor. However, this approach requires a large volume, high cost, and high complexity.[93] The remaining challenges of the above techniques that exploit thinned inorganic materials, inherently soft materials, and extra optical subsystems are resolved by introducing soft structures to device design.

One approach to enhancing the mechanics is the development of concavely curved photodetector arrays with a strain releasing/isolation design (Figure 3d). A thin Si layer on a silicon-on-insulator wafer forms 2D Si photodetector arrays and polyimide films encapsulate the prepared photodetector arrays and mesh-structured metal interconnectors are used for mechanical stability and a passive matrix layout. Transferring the complete device into an elastomeric substrate means that the overall layers including the photodetector array obtain a softness that facilitates 3D deformation. Once the photodetector array transforms into a concave shape, the mesh-structured metal interconnectors allow 3D deformation by releasing/isolating the induced strain (Figure 3f, right).[45,49] Ko et al. fabricated an electronic eye inspired by the human eye based on the

mesh-structured photodetector array scheme (Figure 3e).[45] This study demonstrated an imaging device similar to the human eye with high coverage, curvature, and a single lens. In addition, this scheme enables a RoC-tunable photodetector array by a fluidic instrument that aids variable zoom and excellent imaging characteristics (Figure 3f).[49] One disadvantage is this scheme's low light absorption efficiency due to the ultrathin active medium. Recently, studies for improving the light sensitivity of device in a thin active medium have been attempted by tuning the geometrical parameters and introducing an antireflection coating.[87,95,96]

A kirigami-based device design scheme introduces softness to a photodetector array. In this scheme, a photodetector array with an elaborate petal pattern is fabricated (Figure 3g, left) and then transferred to a concave hemispherical holder (Figure 3g, right). Recently, Wu et al. reported a hemispherical Si-based photodetector array by applying the kirigami method (Figure 3h).[97] Si of thickness <20 μm supplies material flexibility, and the tessellated hexagonal structures enable structural flexibility, both of which help form a hemispherical imager. Therefore, highly deformable photodetector arrays can be fabricated by introducing a kirigami-based design. An appealing feature of this scheme is that it yields high pixel density, which is difficult to realize with a mesh-structure strategy (Figure 3i).

4. Bioinspired Compound Eyes

Compound eyes exhibit numerous strengths and have been the focus of research by optical engineers striving to mimic the design in imaging systems and sensors. There are five classes of compound eye in nature: (1) apposition, (2) reflecting superposition, (3) refracting superposition, (4) parabolic superposition, and (5) neural superposition.[4] The compound eye class differs depending on the creature's residence and active time. Diurnal insects (e.g., bees and dragonflies) usually have the apposition type, which is used in light-sufficient environments. Meanwhile, the superposition type is found in nocturnal arthropods (e.g., moths and fireflies) or crustaceans living in water (e.g., shrimps and lobsters), as these eyes can collect light from adjacent ommatidia to improve light sensitivity. Anatomically, although the detailed structure or mechanism that gathers incoming light differs depending on the type of eye, hemispherically arranged rhabdoms and micro-optics are common features in all compound eyes. In this context, compound eye-inspired systems include the development of micro-optics based on refraction or reflection, and highly curved photodetector arrays correspond to the rhabdoms.

Thus, Subsection 4.1 deals with methods of realizing the focusing micro-optics of two compound eye classes: apposition and reflecting superposition. In addition, an antireflective nanostructure found in nocturnal arthropods is discussed. In Subsection 4.2, we explain the ways of implementing compound eye cameras based on curved photodetector arrays and micro-optics.

4.1. Light-Management Components Inspired by Compound Eyes

Figure 4a is an ommatidium of an apposition compound eye. The ommatidium consists of a crystalline cone containing a lens, rhabdom that absorbs incoming light, and screening layers that block optical crosstalk between each ommatidium. The light that is nearly normal to the ommatidium can be absorbed by a rhabdom, whereas the light at an oblique angle to the ommatidium is blocked by the screening layer. The detailed optical behavior of apposition compound eyes is demonstrated by the 2D emulation of the apposition type (Figure 4a, inset).[98] Photolithographically patterned fluorescent dye (rhodamine 6G) constitutes the 2D layout of the apposition eye to visualize light propagation inside an individual ommatidium. This experimental result clearly shows that the normal incident light to the hemispherical ommatidia array is well guided along an ommatidium, which indicates that a single ommatidium guides the light from an object on a rhabdom. The screening layer obstructs the light from entering adjacent ommatidia. Therefore, this eye anatomy is suitable for environments with sufficient ambient light.

Jeong et al. first fabricated an artificial compound eye that mimicked the apposition-type ommatidium (Figure 4b).[48] Artificial ommatidia consist of a refractive polymer microlens, a polymer cone for guiding the light, and a waveguide for collecting light (Figure 4b, inset). Polymeric microlenses are fabricated using a photosensitive polymer resin. Microlens-assisted photolithography is used for self-writing waveguides, and a photo-/thermal-crosslinking process creates the difference in the refractive indices between the waveguide's core and cladding. The authors also demonstrated that the fabricated ommatidia have similar angular sensitivity levels to the natural eye, where the artificial ommatidium showed values of 1.1°–4.4° compared to bees' natural ommatidium of 1.6°–4.7°.

In addition to the full imitation of apposition compound eye optical units, the microfocusing lenses in the ommatidia of apposition type have been mimicked.[18,99–101] The replica-molding processes have been widely exploited to fabricate polymer-based MLAs. In one successful example, a thermal embossing-based replication process forms a dragonfly eye-inspired PMMA MLA with ≈30 000 ommatidia (Figure 4b).[99] Other strategies explore the fabrication methods of polymer-based curved MLAs using irreversible thermomechanical deformation[102] and self-assembly methods.[103] A recent concept that further enhances the functionality of biological eyes has yielded notable advances in compound eye-inspired optics. The reported strategies include a microdiffractive optics enabling focal length/FoV tuning,[104] graphene-based focal length-tunable microlens array,[105] a liquid crystal-based tunable MLA,[106] a fluid-assisted FoV/focal length-tunable system,[107] and a compound eye lens capable of multispectral imaging.[108]

Research on the reflecting superposition compound eye type has been intense. Unlike the apposition type, this type forms an image on the rhabdom by reflection (Figure 4d), providing robustness to the dispersion of external materials, where the refractive index differs depending on the wavelength. Moreover, reflected or backscattered light from an object is detected by several adjacent ommatidia that gather incoming light and focus it on a rhabdom. This enhances the sensitivity to incoming light (Figure 4d). The pigment-free clear zone that does not hinder light propagation facilitates the superimposing of light from adjacent ommatidia. This compound eye type is the optimal eye anatomy for low-light environments such as

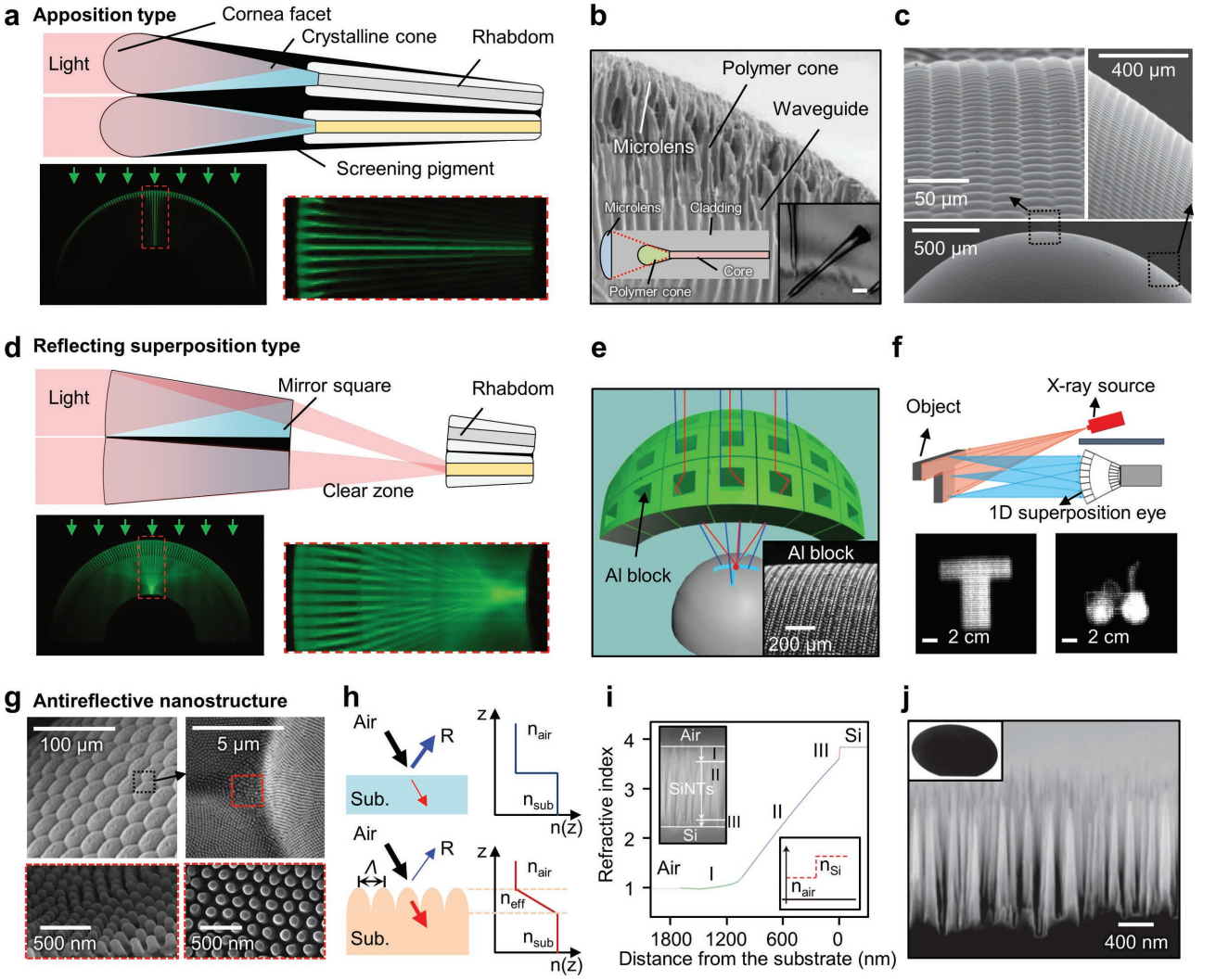

Figure 4. Optical components inspired by compound eyes. a) Schematic of the ommatidium of an apposition compound eye. The inset (Reproduced with permission.[98] Copyright 2012, WILEY-VCH.) shows 2D demonstrations of the apposition compound eye. b,c) Artificial micro-optics of an apposition type eye: (b) Scanning electron microscopy (SEM) image of the ommatidia of an artificial compound eye. The schematic inset shows a single structure and the inset SEM image shows an individual artificial ommatidia; the scale bar is 50 μm. Reproduced with permission.[48] Copyright 2006, American Association for the Advancement of Science. (c) Uniform microlens array. Reproduced with permission.[99] Copyright 2016, WILEY-VCH. d) Schematic of the ommatidium of a reflecting superposition compound eye. The inset (Reproduced with permission.[98] Copyright 2012, WILEY-VCH.) shows 2D demonstrations of the reflecting superposition type. e,f) Man-made reflecting optics that mimic a reflecting superposition eye: (e) Al block array for the reflecting superposition type. Reproduced with permission.[50] Copyright 2014, WILEY-VCH. (f) X-ray-backscattering inspection based on a 1D reflecting superposition eye and obtained images. Reproduced with permission.[109] Copyright 2016, American Institute of Physics. g) SEM images of an *Attacus atlas* compound eye with antireflective nanostructures. Reproduced with permission.[110] Copyright 2011, RSC Publishing. h) Schematic illustration of light reflections and refractive index profiles for the instances of bare material and antireflective nanostructure-coated material. i) Gradient refractive index profile simulation of the surface with biomimetic silicon nanotips (SiNTs). Reproduced with permission.[112] Copyright 2007, Nature Publishing Group. j) SEM image of the SiNTs on the Si wafer. The inset is a photographic image that shows the wafer coated with Si antireflective nanostructures. Reproduced with permission.[112] Copyright 2007, Nature Publishing Group.

underwater or at night.[4] The demonstration of the reflecting superposition type is conducted by the 2D layout of fluorescent dye (Figure 4d, inset);[98] the magnified images clearly display that the superposition type can have strong light by collecting light from adjacent ommatidia.

One route to mimicking the reflecting superposition eye is to integrate a micromirror block array and an elastomeric polymer, thus permitting deformation (Figure 4e).[50] Al-coated sidewalls of Si microsquare tubes serve as microreflecting optics. Subsequent fabrication steps such as transferring micro-reflecting optics to an elastomeric polymer and deforming the overall layers into a hemisphere produce artificially curved reflecting superposition optics (Figure 4e, inset); this allows optical features such as a wide FoV, low chromatic aberration, and enhanced light sensitivity. In particular, a recent study achieved a wavelength-free imaging property of the reflecting superposition type by applying a 1D layout of reflecting superposition optics in the X-ray region (Figure 4f).[109] Such

remarkable imaging features of the reflecting compound eye optics can be exploited in a wide range of applications that employ the nonvisible range, for which window materials are scarce.

Compound eyes suggest the fascinating optical feature of excellent antireflection, originating from the tiny structures on the eyes' surface (Figure 4g).[110] Typically, antireflective nanostructures are found in the eyes of nocturnal creatures such as moths and efficiently collect light in low ambient light environments. Tapered nanostructures are considered a homogenous layer with a continuous refractive index variation (Figure 4h). Strong reflectance occurs when the difference in refractive indices is large, thus a continuous refractive index profile provides the effect of almost zero reflection on a surface. However, achieving an antireflection effect requires that the period (Λ) of the nanostructure is at the subwavelength scale. The index profile can be calculated by the effective medium theory, which is convenient for approximating an optically anisotropic thin films.[111] The effective medium theory is a function of the refractive indices and volume ratios of materials, and the index profile therefore varies along the tapered nanostructures. For instance, the refractive index varies from 1 to that of Si when the exterior material and substrate are air and Si, respectively (Figure 4i).[112] Figure 4j exhibits bioinspired antireflective nanostructures on a Si wafer.[112] The reflectance of these nanostructures remains below 1% and over broadband wavelength ranges, thereby displaying a black color (Figure 4j, inset). This intriguing nanostructure has been widely mimicked for applications in light-emitting devices,[113–115] solar cells,[116–118] and transparent windows[119,120] and the detailed structural features and fabrication methods have been reported in several articles.[111,121–124]

4.2. Compound Eye Imaging Devices

A major challenge in compound eye imaging devices is the implementation of highly curved photodetector arrays and the integration of a photodetector array with micro-optics. The techniques described in Subsections 3.2 and 4.1 establish a basis for the development of compound eye-inspired cameras. Meanwhile, before the emergence of curved photodetector arrays, numerous planar compound eye cameras using wafer-based image sensors have been studied to employ the strengths of compound eyes (e.g., the small form-factor and individual imaging capability).[125–130] This subsection briefly describes the fundamental architecture and features of planar compound eye cameras and discusses the raw materials, mechanics, and optical properties of recently introduced 3D compound eye cameras.

A planar compound eye camera includes an MLA with a short focal length and a separation layer to prevent optical crosstalk that facilitates individual imaging and small-form architecture (**Figure 5**a). However, although it offers such desirable features, this scheme suffers from a severely restricted FoV. Various approaches to widen the FoV such as the manipulation of the microlens shape,[125] employing a multilayered microlens,[131] and using additional optics[132] have been reported. One study on a planar compound eye camera uses a microprism to widen the FoV (Figure 5b) and has a tiny camera layout (Figure 5c).[53] Each microlens obtains images that differ slightly depending on the location of the microlens (Figure 5d). Despite efforts to widen the FoV, further enhancement is required for an omnidirectional sensing compound eye camera (for example, the widest reported FoV is $115° \times 86°$[126]).

One strategy to widen the FoV without complicated optical elements involves a sliced CMOS image sensor along one direction, a flexible printed circuit board (FPCB) utilized as both a flexible substrate and signal readout circuit, and a polymeric MLA with an aperture that permits forming an image (Figure 5e). Vision Tape, which is composed of eight photodiodes on a FPCB, has been demonstrated as a prototype (Figure 5f).[133] The main objective of Vision Tape is to detect objects and provide proximity estimation based on the optical flow method. An enhanced version of this scheme, a cylindrically wide FoV ($180° \times 60°$) imager called "curved artificial compound eye" (CurVACE), has been implemented, as shown in Figure 5g.[51] Exploiting a CMOS chip with a photodetector instead of photodiodes increases the pixel/lens density to 630, which significantly enhances the resolution. In addition, CurVACE yields a 300 Hz signal acquisition bandwidth, which is three times higher than that of fast-flying insects.[51] However, this unidirectionally curved compound eye sensor still cannot provide a hemispherically wide FoV.

One route to a 3D compound eye camera with omnidirectional views is based on the assembly of an elastomeric MLA and stretchable electronics. In such a scheme, thin Si phototransistors consisting of a photodiode and a blocking diode form a photodetector array in an open mesh configuration with matrix addressing. Serpentine-structured metals encapsulated by polyimide serve as electrical and mechanical interconnectors between each pixel. Polydimethylsiloxane (PDMS) MLA fabricated by a molding process and light-screening layer constitutes an optical subsystem. The integration of the two subsystems and deformation yield a hemispherical compound eye camera (Figure 5h). Figure 5i highlights a successful example of this that achieves intriguing imaging features observed in an apposition compound eye, such as individual imaging, an almost hemispherical FoV (160°), a nearly infinite depth of field, and low aberrations.[46] The MLA is based on an elastomeric polymer, and the photodetector array employs stretchable electrodes and thus displays a much lower induced strain than their fracture strain as a result of the mechanical softness of the elastomer and the soft structural device design (Figure 5j).

Recent technological advances in 3D/micro-optical elements and flexible/stretchable electronics based on soft materials and structures have promoted the fabrication of hemispherical compound eye cameras that provide imaging performance found in natural compound eyes. The next research direction is to expand the classes of biomimetics to those found in nature such as other superposition types or different species with hemispherical supporting substrates.[4] Another research direction might be the imitation of the environment-adaptation compound eye to adjust the amount of incoming light, which is observed in some compound eyes.[4] Although the adapting compound eye requires a feedback system that informs about the state of ambient light, it can be used as a day/night imaging device. Simultaneously, further advances should be made to address the remaining challenges of current research, such

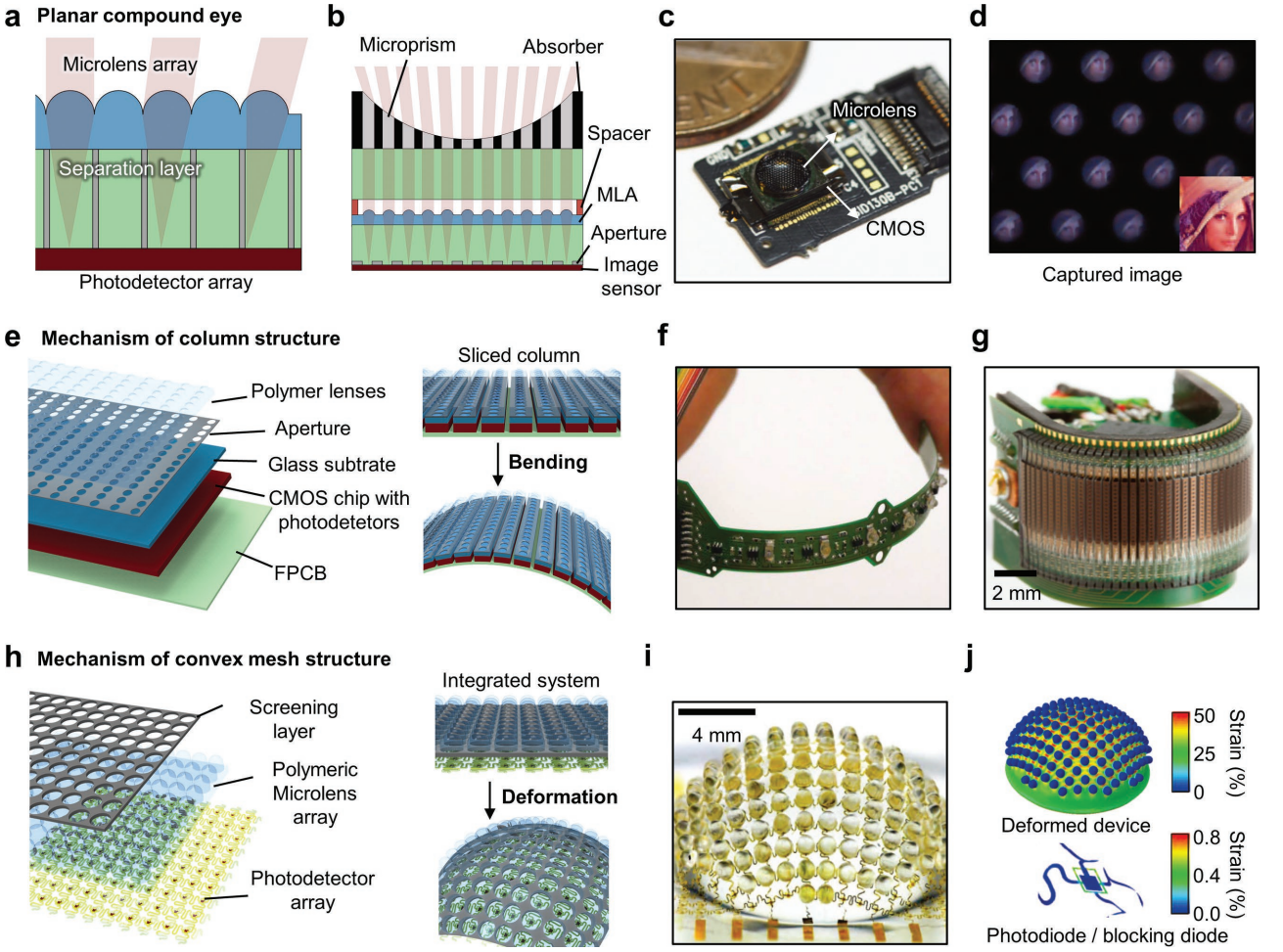

Figure 5. Biomimicry of compound eyes. a) Fundamental architecture of the planar compound eye system. b–d) Layout and optical images of a planar compound eye camera with a microprism. (b) Schematic illustration of the structure. (c) Photograph of a planar compound eye camera. Reproduced with permission.[53] Copyright 2016, IEEE. (d) An image captured using the camera. Reproduced with permission.[53] Copyright 2016, IEEE. e) Schematic illustration of the sliced column structure composed of the FPCB, commercial CMOS sensor, and polymeric lens array. f) An image of Vision Tape, a cylindrical compound eye camera with low pixel density. Reproduced with permission.[133] Copyright 2012, IEEE. g) High-resolution cylindrical vision sensor, CurVACE, fabricated in a column structure. Reproduced with permission.[51] Copyright 2013, National Academy of Sciences. h) Schematic illustration of a hemispherical compound eye camera based on the convex photodetector array method. i,j) Optical image and mechanical simulations of a hemispherical compound eye camera. (i) Photograph of a compound eye camera. Reproduced with permission.[46] Copyright 2013, Nature Publishing Group. (j) Mechanical properties of the polymeric microlens array (top) and single photodiode/blocking diode cell (bottom). Reproduced with permission.[46] Copyright 2013, Nature Publishing Group.

as the problem of low resolution. Opportunities also exist to extend the concepts described above to the mechanical deformation of high-density photodetector arrays or to exploit digital signal processing techniques.[134]

5. Bioinspired Visual Prostheses

People usually recognize objects through vision, but patients with ocular diseases have perception difficulties,[135] which provides strong motivation to develop prosthetic device technologies[35] with which to treat ocular diseases[136] and complement diminished visual function.[19,137] Recently, many studies have presented the meaningful development of novel visual prostheses and progress in the treatment of ocular diseases,[138] from treating retinal degeneration[20,138] (e.g., macular degeneration or retinitis pigmentosa) to ultimately attempting to restore human vision. Retinal prostheses are prominent among the several types of visual prostheses as they present two advantages: relatively easy surgery and intuitive retinal mapping.[25] Retinal prostheses mimic the retina's functions, and thus consist of an image sensor array for recognizing incoming light, cointegrated electronics for processing optical information and generating programed electrical pulses, and a microelectrode array for electrically stimulating optic nerves. Notable technological innovations regarding each component have led to the application of retinal prostheses in the clinical treatment of retina degradation.

Despite these advances, previous approaches have only been able to mimic certain limited functions of the retina and still have bulky sizes and mechanical mismatches

with tissue owing to the rigidity of optoelectronic devices. Applying recently emerging bioinspired technologies[28] permits unconventional electronic and optoelectronic devices to harmonize with soft biological tissues, providing enhanced functionality and user comfort.[139–141] In this context, the field of visual prosthetics should seek to implement more retina-like prostheses by introducing bioinspired technologies. The following subsections briefly introduce the principles of light recognition and visual prostheses. Then, visual prostheses that can mimic the structure and function of the human eye, including a self-powered photovoltaic retinal prosthesis, are described.

5.1. Principles of Light Recognition and Visual Prosthesis

The retina's neurons recognize light and convert it into neural signals. The retina is composed of three layers: an outer nuclear layer (ONL), an inner nuclear layer (INL), and a ganglion cell layer (GCL) (**Figure 6**a).[136] Cones and rods, which are well-known photoreceptor cells, are distributed in the ONL, the INL contains horizontal cells, bipolar cells, and amacrine cells that transmit neural signals to the GCL, and the GCL has retinal ganglion cells (RGCs) that receive the signals from the bipolar cells and transmit action potentials to the visual cortex via the optic nerves. Figure 6b illustrates the mechanism by which

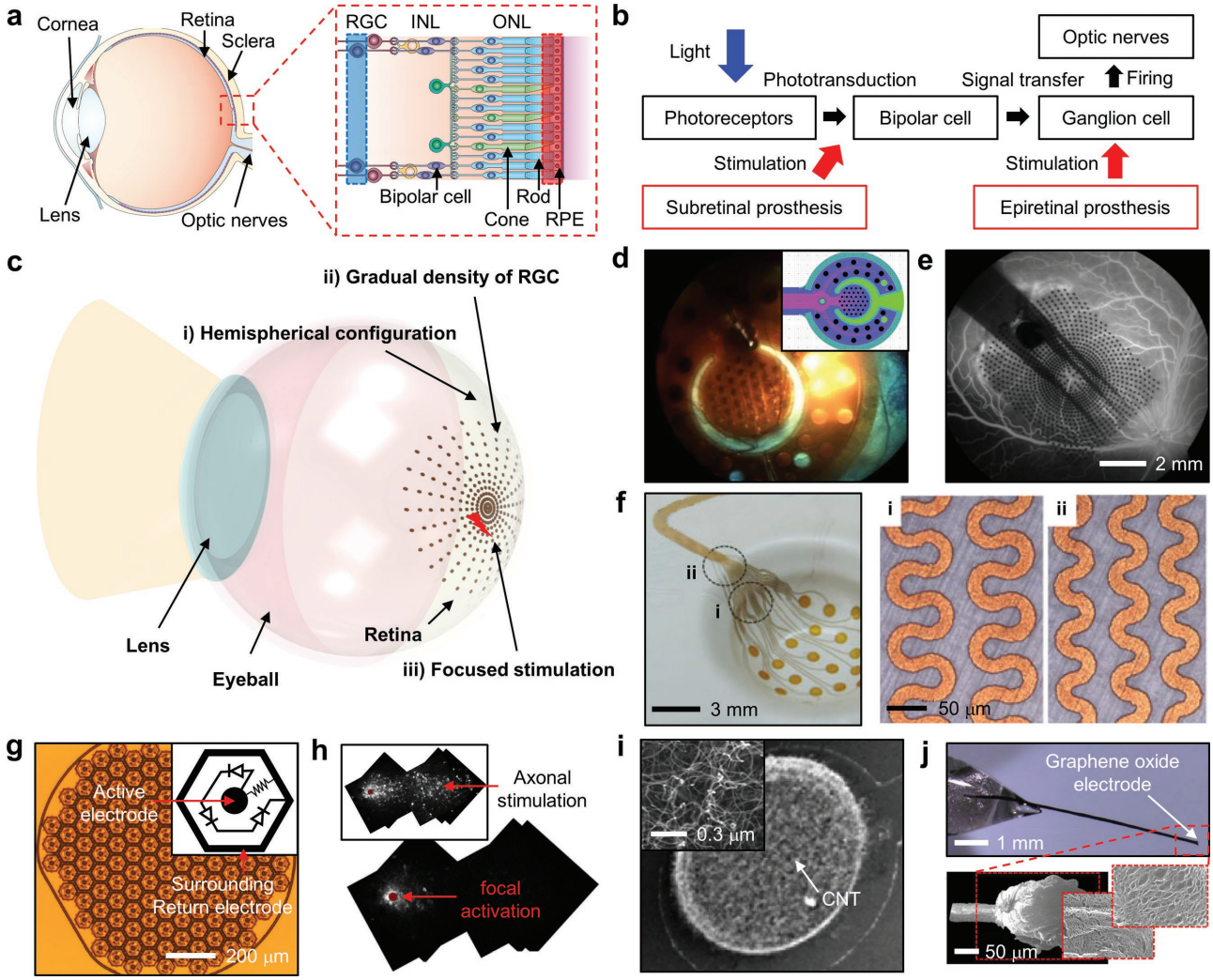

Figure 6. Bioinspired visual prosthesis. a) Structure of the eye and retina. Reproduced with permission.[136] Copyright 2012, Nature Publishing Group. b) Block diagram showing the principles of light recognition. c) Schematic illustration of the human eye's major structural and functional components. d) Photograph of the polyimide device array with origami structure that covers a large area of the hemispherical retina. The inset shows the planar device design prior to deformation. Reproduced with permission.[148] Copyright 2009, IEEE. e) Optical microscope image of a 1 μm thick electrode using parylene. Reproduced with permission.[148] Copyright 2009, IEEE. f) Optical camera image of a polymeric implant with wavy metal tracks that provide stretchability. Reproduced with permission.[152] Copyright 2015, IEEE. g) Photograph of a subretinal prosthesis that gains high visual acuity by blocking the spread of stimulation. The inset shows the wiring diagram for each pixel. Reproduced with permission.[22] Copyright 2015, Nature Publishing Group. h) Image of a locally activated retina. The inset shows the activated retina by unintended axonal stimulation. Reproduced with permission.[23] Copyright 2015, American Association for the Advancement of Science. i) SEM image of an electrode with deposited CNTs. Reproduced with permission.[156] Copyright 2017, Elsevier. j) Optical camera image (top) and SEM image (bottom) of an electrode coated with graphene oxide. Reproduced with permission.[157] Copyright 2015, WILEY-VCH.

light is recognized by retinal neurons.[137] Photoreceptor cells in the ONL convert the incoming light into electrical and chemical signals through phototransduction. The generated signal is transferred to the RGC via the INL's bipolar cells. The RGC collects visual information obtained by various photoreceptors, analyzes and processes this information, and then fires the optic nerves.

In retinal degeneration such as macular degeneration and retinitis pigmentosa, some or all retinal neurons, such as photoreceptor cells, bipolar cells, and RGCs lose functionality and the patient thus becomes blind.[135] The most seriously degraded retinal neuron type determines the suitable visual prosthesis mode, which can be classified into two groups by the implanted position in the retina (Figure 6b).[138] Visual prostheses are classified as follows[19]: (i) an epiretinal prosthesis that is attached to the GCL to directly stimulate the RGC (blue dashed box in Figure 6a, right)[142,143] and (ii) a subretinal prosthesis that is inserted between the ONL and retinal pigment epithelium to stimulate the bipolar cells (red dashed box in Figure 6a, right).[144,145] These two types of visual prosthesis are applied via clinical treatment and lead to improved vision in daily life.[134,136] Additional detailed information about epiretinal and subretinal prostheses can be found in other review papers.[19,146]

5.2. Recent Advances in Bioinspired Visual Prostheses

Bioinspired device design strategies that mimic the structure of mammalian eyes have recently been proposed such as a hemispherical device array configuration for a wider FoV and improved biocompatibility (Figure 6c(i))[22,23,147] and the gradual arrangement of the electrode array to match the density of RGC near the fovea (Figure 6c(ii)).[148] Retinal neurons are widely distributed over the large area of the hemispherical eye, which offers a wider FoV and hence provides better efficacy, user convenience, and mobility.[24,25] However, most conventional retinal prostheses only cover a small area of the retina near the fovea, and the FoV is thus quite limited.[28] While the retina consists of extremely low modulus tissues, conventional devices are stiff.[149] This mechanical mismatch restricts the wide FoV, because a large-size rigid and flat device can easily damage retinal tissue.[150] Bioinspired strategies such as a hemispherically curved device design and soft-form devices[142,151] can provide biocompatible interfaces between soft retinal tissues and the retinal implants.[34] One strategy is to apply a polyimide device with an origami structure that achieves a hemispherical configuration similar to the shape of the human eye to cover a large area of the retina (Figure 6d).[24,148] This device design allows conformal integration of the device with the retina with minimal tissue deformation.[148] Second, a retinal implant based on 1 μm thick parylene has also been fabricated (Figure 6e).[148] The ultrathin implant reduces damage to the retina and allows good integration with the blood vessels near the implant. In addition, gradual arrangement of the electrode array that matches with the gradual density of the RGC near the fovea can improve resolution of retinal stimulation. Another strategy exploits a liquid-crystal polymer (LCP) to fabricate a miniaturized and eye-conformable retinal implant.[152] The LCP provides a waterproof substrate and encapsulation. Thermal deformation of the LCP allows conformal integration of the curved device (Figure 6f). The wavy metal track provides stretchability, minimizing the mechanical stress (Figure 6f(i,ii)).[152,153]

The human eye is capable of seeing objects clearly because of its high visual acuity by focused retinal stimulation (Figure 6c(iii)). Similarly, the goal of bioinspired visual prostheses is to mimic the retina's function and ultimately serve as a close artificial vision of an intact human retina. In this regard, high visual acuity is a vital factor in visual prostheses.[28] One way of increasing visual acuity is selectively stimulating specific retinal neurons within a small area.[150] However, even when using a small-sized electrode, the spread of the stimulating electrical current to nearby neurons prohibits the focal activation of specific retinal neurons;[23] recent advances in electrode designs have addressed this issue (Figure 6g).[22] A return electrode surrounding the active electrode prevents the spread of electrical stimulation and interference with adjacent electrodes by blocking the signal path (Figure 6g, inset). This retinal prosthesis can distinguish a 70 μm spot size, equal to the size of the comprising pixel, and has a Snellen acuity of 20/250, which means that people with such implants need to be 20 ft away to recognize an object that healthy people can see at 250 ft away. In the epiretinal prosthesis, RGC stimulation causes unintended axonal stimulation that spreads the stimulation signal over a large area (Figure 6h, inset). Weitz et al. inhibited axonal stimulation by applying long duration electrical pulses.[23] The increased pulse duration allows for the intensive stimulation of the inner retinal neurons while avoiding the activation of ganglion cell axons (Figure 6h). Thus, retinal stimulation using 25 ms duration pulses achieves a 20/312 Snellen acuity. Nanomaterials offer ways to improve biocompatibility[154] and stimulation efficiency,[155] which affect visual acuity. The deposition of carbon nanotubes (CNTs) onto electrodes leads to the formation of structurally and immunohistochemically excellent interfaces with the retina, reducing the retinal stimulation threshold (Figure 6i).[156] In this method, electrodes coated with a hybrid of poly(3,4-ethylenedioxythiophene) (PEDOT) and CNTs achieve extremely low thresholds (0.0159 mC cm^{-2}) for stimulating the RGC. As another example of nanomaterials, graphene oxide provides the electrode with enhanced charge injection capability.[150] In one published example, an electrode coated with graphene oxide exhibits increased charge injection capacity (46 mC cm^{-2}), which is 200 times greater than that of a platinum electrode and hence effectively stimulates the RGC (Figure 6j).[157]

Despite these advances, further development is still required to develop a visual prosthesis closer to real human vision, such as a soft form device that mechanically matches with soft retinal tissue, improved visual acuity with focused stimulation, better color recognition, and binocular vision realization. First, optic nerves are widely distributed over the soft and hemispherical retina, hence they can be easily damaged by stiff implanted devices. Soft optoelectronic/electronic device with similar mechanical properties to retinal tissues could be a promising candidate of such visual prostheses due to their minimal mechanical mismatch.[139] Second, the visual acuity of conventional visual prostheses remains much worse than that of an intact human eye;[22] thus, higher-resolution retinal

stimulation without the spread of the electrical stimulation using the higher-density pixels of photodetectors and electrodes is required. In addition to the visual acuity, conventional retinal prostheses cannot recognize actual color, because they cannot selectively stimulate individual color-specific neurons, which are generally much smaller than the size of safe stimulation (<50 μm).[19] Recognizing color requires focused stimulation within an area smaller than the diameter of each spectrally specific neuron.[19] Finally, the bulky hardware of current visual prostheses such as head-mounted cameras[142] hinders the binocular vision that facilitates better depth detection, wider FoV, and binocular summation because of the mismatch between vision acquired through a head-mounted camera and vision obtained via stimulated retinal neurons. In a healthy retina, the photoreceptor cells absorb incident light and generate neural signals by themselves, and thus there is no mismatch between the position the light has illuminated and the position where the retinal neurons are activated. Therefore, a similar device design that places the photodetector and stimulation electrode in the same position could be a good approach to resolving this issue. For example, Alpha-IMS integrates a photodetector, integrated electronics, and an electrode in an individual pixel.[19,144]

5.3. Self-Powered Visual Prosthesis Using Photovoltaic Devices

The intraocular cables in most conventional visual prostheses accompany a high risk of inflammatory reactions and limited pixel density due to the wiring.[158] In this context, the most important factor for developing next-generation visual prosthesis is a wireless system that can supply power and transmit signals wirelessly. Although visual prostheses using wireless communication technology have been reported,[159] this scheme still requires microchips and cables to receive external electromagnetic waves.

Retinal neurons can be activated by receiving incoming light; similarly, self-powered visual prostheses that employ Si photovoltaic devices that generate current by receiving photons have been recently developed.[22,27,159] A camera in head-mounted glasses detects an external image, and an image processor generates infrared (IR) light of the same image, which it transfers to the Si photovoltaic devices implanted in the subretina (**Figure 7**a).[160] The Si photovoltaic component receives the wirelessly transmitted pulsed IR light, generates a corresponding charge-balanced pulse, and stimulates the retina (Figure 7b). This strategy exploits light instead of electrical signals as a medium for signal transmission, and hence facilitates

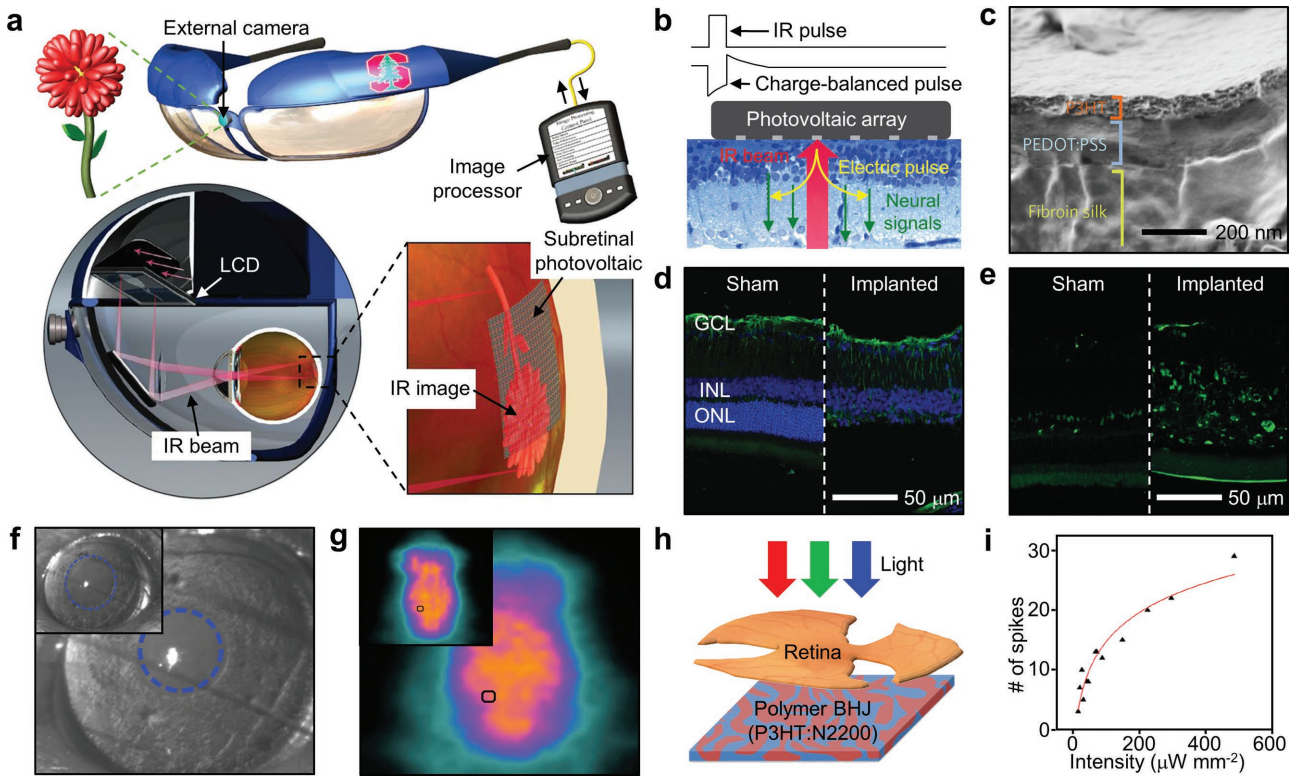

Figure 7. Wireless and self-powered subretinal prosthesis that uses photovoltaics. a) A schematic image showing how the photovoltaic retinal prosthesis works. Reproduced with permission.[160] Copyright 2012, Nature Publishing Group. b) Schematic image of the photovoltaic retinal prosthesis; the photovoltaic retinal prosthesis generates a charge-balanced pulse upon receiving an IR beam. Reproduced with permission.[160] Copyright 2012, Nature Publishing Group. c) Scanning microscope image of an organic-based photovoltaic retinal prosthesis. Reproduced with permission.[26] Copyright 2017, Nature Publishing Group. d,e) (d) GFAP and (e) FGF expression of a sham-operated retina and a retina with an implanted device. Reproduced with permission.[162] Copyright 2016, WILEY-VCH. f,g) (f) Recovered pupil responses and (g) reactivated metabolism of the visual cortex by implanting the photovoltaic retinal prosthesis for six to ten months. The inset of (g) shows the metabolism of a healthy mouse's visual cortex. Reproduced with permission.[26] Copyright 2017, Nature Publishing Group. h) Schematic image of the photovoltaic retinal prosthesis using a polymer bulk heterojunction. Reproduced with permission.[163] Copyright 2014, WILEY-VCH. i) Graphs showing the number of neural spikes generated by external light. Reproduced with permission.[163] Copyright 2014, WILEY-VCH.

wireless retinal stimulation without complicated electronics and wires. However, such subretinal implants require 30 μm thick rigid flat Si membranes to absorb sufficient light, which causes severe mechanical deformation in the softly curved retina;[27] therefore, it cannot cover a large area of the retina.

Photovoltaic retinal prostheses that use soft organic materials have been developed as a solution (Figure 7c).[26,161,162] Such photovoltaic prostheses consist of a fibroin silk substrate, a poly(3-hexylthiophene) (P3HT) photoabsorbing layer, and a PEDOT:polystyrene charge transfer layer. The overall thickness is <1 μm, and the organic materials of which it is comprised are intrinsically soft.[29,140] A retina implanted with organic-based devices shows good biocompatibility, as shown in the results of glial fibrillary acidic protein (GFAP) expression (Figure 7d) and fibroblast growth factors (FGFs) (Figure 7e), similar to those of a sham-operated retina.[162] Increased GFAP immunoreactivity represents retinal stress by foreign bodies.[162] The upregulated expression of FGFs is an indicator of mechanical stress between the retina and the vitreous gel.[162] In short, ultrathin device thickness and the use of soft materials improve the biocompatibility of the retinal implants. The long-term (six to ten months) implantation of an organic-based device into the subretina of retina-degenerated (RD) mice recovers the function of the degenerated eye.[26] The implanted photovoltaic devices substitute the role of degraded photoreceptors, stimulating the retina by receiving external light and long-term retinal stimulation restores the pupil response in RD mice (Figure 7f). In addition, the visual cortex's metabolism in RD mice was reactivated to a similar level to that of healthy mice (Figure 7g).

Photovoltaic retinal prostheses require intense light to generate an adequate number of electrical pulses to stimulate the retina, but a high-intensity light beam can increase the temperature and cause serious side effects. A photovoltaic retinal prosthesis has been developed to address this issue using an organic bulk heterojunction that increases the sensitivity and generates sufficient current, even in low-intensity light.[163] One example using a bulk heterojunction of P3HT:N2200 showed the successful generation of strong electrical pulses by receiving low-intensity light (Figure 7h). The device could generate spikes with the light of 100 μW mm^{-2} intensity (Figure 7i).

6. Conclusion and Perspective

Many scientists and engineers have continuously pursued mimicry of biological eyes to implement optically outstanding and remarkably compact imaging devices. These efforts have resulted in significant progress in the imaging industries as well as emerging fields such as robotics, biomedicine, and photonics. The foremost aspiration is to provide a new design paradigm that mimics the strategies of the human eye and ingenious sensory systems inspired by insects. Recent progress in bioinspired imaging systems has yielded broad technological advances, including the development of a single-lens system beyond conventional complicated multiple lenses, new imaging schemes that capture panoramic views without optical aberrations with a small form-factor, almost no wavelength-limitation for focusing elements, and advanced light-management elements. Soft materials and deformable device technologies have underpinned these achievements by providing the potential to realize particular architectures inspired by animal eyes. Unique features of biological eyes are reflected in artificial eyes' flexible, stretchable, and 3D structures.

Although the bioinspired imaging systems have shown dramatic recent progress, visual prosthesis technologies have been developing more slowly. However, recent advances in soft electronics, optoelectronics, and human eye-inspired system designs have led to significant improvements in visual prostheses, such as enhanced visual acuity, widened FoV, and the achievement of biocompatible interfaces between soft retinal tissues and implanted devices. Self-powered soft retinal prostheses based on photovoltaic devices can operate without immune responses over a long period of time and intriguing curved systems that restore the function of degenerated retina in a mouse model and have received attention as a candidate for next-generation visual prostheses. In addition, further advances are needed to achieve soft and biocompatible retinal implants, increase the FoV of visual prostheses, implement high-density pixels, and apply focused stimulation.

In summary, foundational research that mimics biological eyes encompasses the development of exceptional optical subcomponents and the implementation of innovative imaging devices. Furthermore, the emulation of biological eyes has led to advances in human eye-like visual prosthesis technologies. These research activities will continue ranging from the basic structural imitation of animal eyes to perfect replication of natural visual capabilities. Thus far, impressive progress has been achieved in bioinspired artificial eyes through the biomimicry of two types of eyes: human and apposition. Biological eyes that have not yet been perfectly mimicked but their structures are known offer strong potential for applications that require extraordinary optical and photonic features such as the hyperacuity of rapacious birds,[79] scotopic vision of superposition eyes,[12,59] and polarization/multispectral imaging of shrimp eyes.[164,165] Furthermore, with mature man-made technologies, adding functionality to bioinspired devices can open new directions for next-generation imaging devices. The inexhaustible applicability of bioinspired technology is in line with the recent production trends of industries' "multi-item small-sized production" that seeks multifunctional and multidesigned products, and this feature will provide many opportunities in the field of robot eyes and visual prostheses.

Acknowledgements

G.J.L. and C.C. contributed equally to this work. This research was supported by the Creative Materials Discovery Program through the National Research Foundation of Korea (NRF) funded by the Ministry of Science and ICT (NRF-2017M3D1A1039288). This work was also supported by IBS-R006-A1.

Conflict of Interest

The authors declare no conflict of interest.

Keywords

bioinspired imaging systems, flexible electronics, soft materials, stretchable electronics, visual prostheses

Received: September 10, 2017
Revised: October 28, 2017
Published online: December 18, 2017

[1] D. Atchison, G. Smith, *Optics of the Human Eye*, Butterworth-Heinemann, Oxford, UK **2000**.
[2] C. Posch, T. Serrano-Gotarredona, B. Linares-Barranco, T. Delbruck, *Proc. IEEE* **2014**, *102*, 1470.
[3] J. Ahn, C.-R. Moon, B. Kim, K. Lee, Y. Kim, M. Lim, W. Lee, H. Park, K. Moon, J. Yoo, Y. Lee, B. Park, S. Jung, J. Lee, T.-H. Lee, Y. Lee, J. Jung, J.-H. Kim, T.-C. Kim, H. Cho, D. Lee, Y. Lee, in *IEEE Int. Electron Devices Meeting*, IEEE, San Francisco, CA, USA **2008**, p. 1.
[4] M. F. Land, D. Nilsson, *Animal Eyes*, Oxford University Press, Oxford, UK **2012**.
[5] L. P. Lee, R. Szema, *Science* **2005**, *310*, 1148.
[6] G. Zhou, H. Yu, Y. Du, F. S. Chau, *Opt. Lett.* **2012**, *37*, 1745.
[7] C. G. Tsai, J. A. Yeh, *Opt. Lett.* **2010**, *35*, 2484.
[8] F. Carpi, G. Frediani, S. Turco, D. De Rossi, *Adv. Funct. Mater.* **2011**, *21*, 4152.
[9] J. Y. An, J. H. Hur, S. Kim, J. H. Lee, *IEEE Photonics Technol. Lett.* **2011**, *23*, 1703.
[10] L. Dong, A. K. Agarwal, D. J. Beebe, H. Jiang, *Nature* **2006**, *442*, 551.
[11] L. Li, C. Liu, Q.-H. Wang, *IEEE Photonics Technol. Lett.* **2013**, *25*, 989.
[12] M. F. Land, *Contemp. Phys.* **1988**, *29*, 435.
[13] V. Lakshminarayanan, M. K. Parthasarathy, *J. Mod. Opt.* **2016**, *9*, 1.
[14] H. Jung, K. Jeong, *Opt. Express* **2009**, *17*, 14761.
[15] H. K. Raut, S. S. Dinachali, Y. C. Loke, R. Ganesan, K. K. Ansah-Antwi, A. Góra, E. H. Khoo, V. A. Ganesh, M. S. M. Saifullah, S. Ramakrishna, *ACS Nano* **2015**, *9*, 1305.
[16] Y. W. Kwon, J. Park, T. Kim, S. H. Kang, H. Kim, J. Shin, S. Jeon, S. W. Hong, *ACS Nano* **2016**, *10*, 4609.
[17] S. Ji, J. Park, H. Lim, *Nanoscale* **2012**, *4*, 4603.
[18] H. Jung, K.-H. Jeong, *Appl. Phys. Lett.* **2012**, *101*, 203102.
[19] E. Zrenner, *Sci. Transl. Med.* **2013**, *5*, 210ps16.
[20] R. K. Shepherd, M. N. Shivdasani, D. A. X. Nayagam, C. E. Williams, P. J. Blamey, *Trends Biotechnol.* **2013**, *31*, 562.
[21] H. Nazari, P. Falabella, L. Yue, J. Weiland, M. S. Humayun, *J. Vitreoretin. Dis.* **2017**, *1*, 204.
[22] H. Lorach, G. Goetz, R. Smith, X. Lei, Y. Mandel, T. Kamins, K. Mathieson, P. Huie, J. Harris, A. Sher, D. Palanker, *Nat. Med.* **2015**, *21*, 476.
[23] A. C. Weitz, D. Nanduri, M. R. Behrend, A. Gonzalez-Calle, R. J. Greenberg, M. S. Humayun, R. H. Chow, J. D. Weiland, *Sci. Transl. Med.* **2015**, *7*, 318ra203.
[24] H. Ameri, T. Ratanapakorn, S. Ufer, H. Eckhardt, M. S. Humayun, J. D. Weiland, *J. Neural Eng.* **2009**, *6*, 035002.
[25] J. Villalobos, D. A. X. Nayagam, P. J. Allen, P. McKelvie, C. D. Luu, L. N. Ayton, A. L. Freemantle, M. McPhedran, M. Basa, C. C. McGowan, R. K. Shepherd, C. E. Williams, *Invest. Ophthalmol. Visual Sci.* **2013**, *54*, 3751.
[26] J. F. Maya-Vetencourt, D. Ghezzi, M. R. Antognazza, E. Colombo, M. Mete, P. Feyen, A. Desii, A. Buschiazzo, M. D. Paolo, S. D. Marco, F. Ticconi, L. Emionite, D. Shmal, C. Marini, I. Donelli, G. Freddi, R. Maccarone, S. Bisti, G. Sambuceti, G. Pertile, G. Lanzani, F. Benfenati, *Nat. Mater.* **2017**, *16*, 681.
[27] Y. Mandel, G. Goetz, D. Lavinsky, P. Huie, K. Mathieson, L. Wang, T. Kamins, L. Galambos, R. Manivanh, J. Harris, D. Palanker, *Nat. Commun.* **2013**, *4*, 1980.
[28] D. Ghezzi, *Front. Neurosci.* **2015**, *9*, 290.
[29] T.-M. Fu, G. Hong, T. Zhou, T. G. Schuhmann, R. D. Viveros, C. M. Lieber, *Nat. Methods* **2016**, *13*, 875.
[30] T. Tokuda, Y. Takeuchi, Y. Sagawa, T. Noda, K. Sasagawa, K. Nishida, T. Fujikado, J. Ohta, *IEEE Trans. Biomed. Circuits Syst.* **2010**, *4*, 445.
[31] G. Shin, I. Jung, V. Malyarchuk, J. Song, S. Wang, H. C. Ko, Y. Huang, J. S. Ha, J. A. Rogers, *Small* **2010**, *6*, 851.
[32] K.-I. Jang, H. U. Chung, S. Xu, C. H. Lee, H. Luan, J. Jeong, H. Cheng, G.-T. Kim, S. Y. Han, J. W. Lee, J. Kim, M. Cho, F. Miao, Y. Yang, H. N. Jung, M. Flavin, H. Liu, G. W. Kong, K. J. Yu, S. I. Rhee, J. Chung, B. Kim, J. W. Kwak, M. H. Yun, J. Y. Kim, Y. M. Song, U. Paik, Y. Zhang, Y. Huang, J. A. Rogers, *Nat. Commun.* **2015**, *6*, 6566.
[33] Y. Ma, K.-I. Jang, L. Wang, H. N. Jung, J. W. Kwak, Y. Xue, H. Chen, Y. Yang, D. Shi, X. Feng, J. A. Rogers, Y. Huang, *Adv. Funct. Mater.* **2016**, *26*, 5345.
[34] J. Kim, R. Ghaffari, D.-H. Kim, *Nat. Biomed. Eng.* **2017**, *1*, 0049.
[35] J. Kim, M. Lee, H. J. Shim, R. Ghaffari, H. R. Cho, D. Son, Y. H. Jung, M. Soh, C. Choi, S. Jung, K. Chu, D. Jeon, S.-T. Lee, J. H. Kim, S. H. Choi, T. Hyeon, D.-H. Kim, *Nat. Commun.* **2014**, *5*, 5747.
[36] D.-H. Kim, N. Lu, Y. Huang, J. A. Rogers, *MRS Bull.* **2012**, *37*, 226.
[37] T. Yamada, Y. Hayamizu, Y. Yamamoto, Y. Yomogida, A. Izadi-Najafabadi, D. N. Futaba, K. Hata, *Nat. Nanotechnol.* **2011**, *6*, 296.
[38] K. Hata, D. N. Futaba, K. Mizuno, T. Namai, M. Yumura, S. Iijima, *Science* **2004**, *306*, 1362.
[39] X. Yang, C. Cheng, Y. Wang, D. Li, *Science* **2013**, *341*, 534.
[40] S.-M. Lee, J.-H. Kim, J.-H. Ahn, *Mater. Today* **2015**, *18*, 336.
[41] S.-Y. Min, T.-S. Kim, Y. Lee, H. Cho, W. Xu, T.-W. Lee, *Small* **2015**, *11*, 45.
[42] J. Chang, M. Dommer, C. Chang, L. Lin, *Nano Energy* **2012**, *1*, 356.
[43] S. Choi, H. Lee, R. Ghaffari, T. Hyeon, D.-H. Kim, *Adv. Mater.* **2016**, *28*, 4203.
[44] W. Lee, J. Lee, H. Yun, J. Kim, J. Park, C. Choi, D. C. Kim, H. Seo, H. Lee, J. W. Yu, W. B. Lee, D.-H. Kim, *Adv. Mater.* **2017**, *29*, 1702902.
[45] H. C. Ko, M. P. Stoykovich, J. Song, V. Malyarchuk, W. M. Choi, C.-J. Yu, J. B. Geddes, J. Xiao, S. Wang, Y. Huang, J. A. Rogers, *Nature* **2008**, *454*, 748.
[46] Y. M. Song, Y. Xie, V. Malyarchuk, J. Xiao, I. Jung, K.-J. Choi, Z. Liu, H. Park, C. Lu, R.-H. Kim, R. Li, K. B. Crozier, Y. Huang, J. A. Rogers, *Nature* **2013**, *497*, 95.
[47] D.-E. Nilsson, *Visual Neurosci.* **2013**, *30*, 5.
[48] K.-H. Jeong, J. Kim, L. P. Lee, *Science* **2006**, *312*, 557.
[49] I. Jung, J. Xiao, V. Malyarchuk, C. Lu, M. Li, Z. Liu, J. Yoon, Y. Huang, J. A. Rogers, *Proc. Natl. Acad. Sci. USA* **2011**, *108*, 1788.
[50] C.-C. Huang, X. Wu, H. Liu, B. Aldalali, J. A. Rogers, H. Jiang, *Small* **2014**, *10*, 3050.
[51] D. Floreano, R. Pericet-Camara, S. Viollet, F. Ruffier, A. Brückner, R. Leitel, W. Buss, M. Menouni, F. Expert, R. Juston, M. K. Dobrzynski, G. L'Eplattenier, F. Recktenwald, H. A. Mallot, N. Franceschini, *Proc. Natl. Acad. Sci. USA* **2013**, *110*, 9267.
[52] A. Brückner, J. Duparré, R. Leitel, P. Dannberg, A. Bräuer, A. Tünnermann, *Opt. Express* **2010**, *18*, 24379.
[53] D. Keum, D. S. Jeon, C. S. H. Hwang, E. K. Buschbeck, M. H. Kim, K.-H. Jeong, in *Proc. of the IEEE Int. Conf. on Micro Electro Mechanical Systems (MEMS)*, IEEE, Shanghai, China **2016**, p. 636.
[54] S. Ji, M. Ponting, R. S. Lepkowicz, A. Rosenberg, R. Flynn, G. Beadie, E. Baer, *Opt. Express* **2012**, *20*, 151.

[55] S.-B. Rim, P. B. Catrysse, R. Dinyari, K. Huang, P. Peumans, *Opt. Express* **2008**, *16*, 4965.
[56] J. Jang, Y. Yoo, J. Kim, J. Paik, *Sensors* **2015**, *15*, 5747.
[57] G. J. Lee, W. I. Nam, Y. M. Song, *Opt. Laser Technol.* **2017**, *96*, 50.
[58] P. J. Sands, *J. Opt. Soc. Am.* **1971**, *61*, 777.
[59] M. F. Land, *J. Opt. A: Pure Appl. Opt.* **2000**, *2*, 44.
[60] M. F. Land, *Curr. Biol.* **2013**, *23*, 611.
[61] G. Zuccarello, D. Scribner, R. Sands, L. J. Buckley, *Adv. Mater.* **2002**, *14*, 1261.
[62] S. Ji, K. Yin, M. Mackey, A. Brister, M. Ponting, E. Baer, *Opt. Eng.* **2013**, *52*, 112105.
[63] Y.-Y. Zhao, Y.-L. Zhang, M.-L. Zheng, X.-Z. Dong, X.-M. Duan, Z.-S. Zhao, *Laser Photonics Rev.* **2016**, *10*, 665.
[64] S. Petsch, S. Schuhladen, L. Dreesen, H. Zappe, *Light: Sci. Appl.* **2016**, *5*, e16068.
[65] P. M. Moran, S. Dharmatilleke, A. H. Khaw, K. W. Tan, M. L. Chan, I. Rodriguez, *Appl. Phys. Lett.* **2006**, *88*, 041120.
[66] K. Mishra, C. Murade, B. Carreel, I. Roghair, J. M. Oh, G. Manukyan, D. V. D. Ende, F. Mugele, *Sci. Rep.* **2014**, *4*, 6378.
[67] J. W. Bae, E.-J. Shin, J. Jeong, D.-S. Choi, J. E. Lee, B. U. Nam, L. Lin, S.-Y. Kim, *Sci. Rep.* **2017**, *7*, 2068.
[68] M. Pieroni, C. Lagomarsini, D. D. Rossi, F. Carpi, *Bioinspiration Biomimetics* **2016**, *11*, 65003.
[69] L. Maffl, S. Rosset, M. Ghilardi, F. Carpi, H. Shea, *Adv. Funct. Mater.* **2015**, *25*, 1656.
[70] S. Schuhladen, S. Petsch, P. Liebetraut, P. Müller, H. Zappe, *Opt. Lett.* **2013**, *38*, 3991.
[71] S. Schuhladen, F. Preller, R. Rix, S. Petsch, R. Zentel, H. Zappe, *Adv. Mater.* **2014**, *26*, 7247.
[72] P. Müller, R. Feuerstein, H. Zappe, *J. Microelectromech. Syst.* **2012**, *21*, 1156.
[73] S. Schuhladen, K. Banerjee, M. Sturmer, P. Muller, U. Wallrabe, H. Zappe, *Light: Sci. Appl.* **2016**, *5*, e16005.
[74] J. Draheim, T. Burger, J. G. Korvink, U. Wallrabe, *Opt. Lett.* **2011**, *36*, 2032.
[75] H. Zeng, O. M. Wani, P. Wasylczyk, R. Kaczmarek, A. Priimagi, *Adv. Mater.* **2017**, *29*, 1701814.
[76] R. H. H. Kröger, *Prog. Retinal Eye Res.* **2013**, *34*, 78.
[77] W. S. Jagger, *Vision Res.* **1991**, *32*, 1271.
[78] H. Liu, Y. Huang, H. Jiang, *Proc. Natl. Acad. Sci. USA* **2016**, *113*, 3982.
[79] M. P. Jones, K. E. Pierce, D. Ward, *J. Exot. Pet Med.* **2007**, *16*, 69.
[80] F. Xu, W. Huang, J. Liu, W. Pang, *J. Mod. Opt.* **2016**, *63*, 2211.
[81] D. Dumas, M. Fendler, N. Baier, J. Primot, E. L. Coarer, *Appl. Opt.* **2012**, *51*, 5419.
[82] B. Guenter, N. Joshi, R. Stoakley, A. Keefe, K. Geary, R. Freeman, J. Hundley, P. Patterson, D. Hammon, G. Herrera, E. Sherman, A. Nowak, R. Schubert, P. Brewer, L. Yang, R. Mott, G. McKnight, *Opt. Express* **2017**, *25*, 13010.
[83] X. Xu, M. Mihnev, A. Taylor, S. R. Forrest, *Appl. Phys. Lett.* **2009**, *94*, 043313.
[84] X. Xu, M. Davanco, X. Qi, S. R. Forrest, *Org. Electron.: Phys., Mater. Appl.* **2008**, *9*, 1122.
[85] X. Liu, E. K. Lee, D. Y. Kim, H. Yu, J. H. Oh, *ACS Appl. Mater. Interfaces* **2016**, *8*, 7291.
[86] D. Fan, K. Lee, S. R. Forrest, *ACS Photonics* **2016**, *3*, 670.
[87] J.-H. Seo, K. Zhang, M. Kim, D. Zhao, H. Yang, W. Zhou, *Adv. Opt. Mater.* **2015**, *4*, 120.
[88] L. Li, L. Gu, Z. Lou, Z. Fan, G. Shen, *ACS Nano* **2017**, *11*, 4067.
[89] S. Lim, D.-S. Um, M. Ha, Q. Zhang, Y. Lee, Y. Lin, Z. Fan, H. Ko, *Nano Res.* **2017**, *10*, 22.
[90] Deng, X. Zhang, L. Huang, X. Xu, L. Wang, J. Wang, Q. Shang, S.-T. Lee, J. Jie, *Adv. Mater.* **2016**, *28*, 2201.
[91] L. Gu, M. M. Tavakoli, D. Zhang, Q. Zhang, A. Waleed, Y. Xiao, K.-H. Tsui, Y. Lin, L. Liao, J. Wang, Z. Fan, *Adv. Mater.* **2016**, *28*, 9713.
[92] X. Li, D. Yu, J. Chen, Y. Wang, F. Cao, Y. Wei, Y. Wu, L. Wang, Y. Zhu, Z. Sun, J. Ji, Y. Shen, H. Sun, H. Zeng, *ACS Nano* **2017**, *11*, 2015.
[93] I. Stamenov, A. Arianpour, S. J. Olivas, I. P. Agurok, A. R. Johnson, R. A. Stack, R. L. Morrison, J. E. Ford, *Opt. Express* **2014**, *22*, 31708.
[94] Y. Dong, Y. Zou, J. Song, Z. Zhu, J. Li, H. Zeng, *Nano Energy* **2016**, *30*, 173.
[95] M. S. Kim, G. J. Lee, H. M. Kim, Y. M. Song, *Sensors* **2017**, *17*, 1774.
[96] M. Dang, H.-C. Yuan, Z. Ma, J. Ma, G. Qin, *Appl. Phys. Lett.* **2017**, *110*, 253104.
[97] T. Wu, S. S. Hamann, A. C. Ceballos, C.-E. Chang, O. Solgaard, R. T. Howe, *Microsyst. Nanoeng.* **2016**, *2*, 16019.
[98] D. Keum, H. Jung, K.-H. Jeong, *Small* **2012**, *8*, 2169.
[99] Z. Deng, F. Chen, Q. Yang, H. Bian, G. Du, J. Yong, C. Shan, X. Hou, *Adv. Funct. Mater.* **2016**, *26*, 1995.
[100] D. Wu, J.-N. Wang, L.-G. Niu, X. L. Zhang, S. Z. Wu, Q.-D. Chen, L. P. Lee, H. B. Sun, *Adv. Opt. Mater.* **2014**, *2*, 751.
[101] J. Luo, Y. Guo, X. Wang, F. Fan, *J. Micromech. Microeng.* **2017**, *27*, 045011.
[102] H. Liu, F. Chen, Q. Yang, P. Qu, S. He, X. Wang, J. Si, X. Hou, *Appl. Phys. Lett.* **2016**, *100*, 133701.
[103] W.-K. Kuo, S.-Y. Lin, S.-W. Hsu, H. H. Yu, *Opt. Mater.* **2017**, *66*, 630.
[104] M. J. Moghimi, J. Fernandes, A. Kanhere, H. Jiang, *Sci. Rep.* **2015**, *5*, 15681.
[105] L. Wang, F. Li, H. Liu, W. Jiang, D. Niu, R. Li, L. Yin, Y. Shi, B. Chen, *ACS Appl. Mater. Interfaces* **2015**, *7*, 21416.
[106] F. Serra, M. A. Gharbi, Y. Luo, I. B. Liu, N. D. Bade, R. D. Kamien, S. Yang, K. J. Stebe, *Adv. Opt. Mater.* **2015**, *3*, 1287.
[107] K. Wei, H. Zeng, Y. Zhao, *Lab Chip* **2014**, *14*, 3594.
[108] J. Chen, H. H. Lee, D. Wang, S. Di, S.-C. Chen, *Opt. Express* **2017**, *25*, 4180.
[109] J. Xu, X. Wang, Q. Zhan, S. Huang, Y. Chen, B. Mu, *Rev. Sci. Instrum.* **2016**, *87*, 073103.
[110] D.-H. Ko, J. R. Tumbleston, K. J. Henderson, L. E. Euliss, J. M. DeSimone, R. Lopez, E. T. Samulski, *Soft Matter* **2011**, *7*, 6404.
[111] H. Kikuta, H. Toyota, W. Yu, *Opt. Rev.* **2003**, *10*, 63.
[112] Y.-F. Huang, S. Chattopadhyay, Y.-J. Jen, C.-Y. Peng, T.-A. Liu, Y.-K. Hsu, C.-L. Pan, H.-C. Lo, C.-H. Hsu, Y.-H. Chang, C.-S. Lee, K.-H. Chen, L.-C. Chen, *Nat. Nanotechnol.* **2007**, *2*, 770.
[113] L. Zhou, Q.-D. Ou, T.-D. Chen, S. Shen, J.-X. Tang, Y.-Q. Li, S.-T. Lee, *Sci. Rep.* **2014**, *4*, 4540.
[114] G. J. Lee, Y. M. Song, *AIP Adv.* **2016**, *6*, 035104.
[115] Y. M. Song, G. C. Park, S. J. Jang, J. H. Ha, J. S. Yu, Y. T. Lee, *Opt. Express* **2011**,*19*, A157.
[116] Y. M. Song, Y. Jeong, C. I. Yeo, Y. T. Lee, *Opt. Express* **2012**, *20*, A 916.
[117] A. Rahman, A. Ashraf, H. Xin, X. Tong, P. Sutter, M. D. Eisaman, C. T. Black, *Nat. Commun.* **2015**, *6*, 5963.
[118] S. M. Kang, S. Jang, J.-K. Lee, Y. Yoon, D.-E. Yoo, J.-W. Lee, M. Choi, N.-G. Park, *Small* **2016**, *12*, 2443.
[119] S. Ji, K. Song, T. B. Nguyen, N. Kim, H. Lim, *ACS Appl. Mater. Interfaces* **2013**, *5*, 10731.
[120] Y. M. Song, H. J. Choi, J. S. Yu, Y. T. Lee, *Opt. Express* **2010**, *18*, 13063.
[121] J.-Q. Xi, M. F. Schubert, J. K. Kim, E. F. Schubert, M. Chen, S.-Y. Lin, W. Liu, J. A. Smart, *Nat. Photonics* **2007**, *1*, 176.
[122] K. Choi, Y. Yoon, J. Jung, C. W. Ahn, G. J. Lee, Y. M. Song, M. J. Ko, H. S. Lee, B. Kim, I.-S. Kang, *Adv. Opt. Mater.* **2017**, *5*, 1600616.
[123] Y. M. Song, S. J. Jang, J. S. Yu, Y. T. Lee, *Small* **2010**, *6*, 984.

[124] C.-H. Sun, P. Jiang, B. Jiang, *App. Phys. Lett.* **2008**, *92*, 061112.
[125] J. Duparré, P. Dannberg, P. Schreiber, A. Bräuer, A. Tünnermann, *Appl. Opt.* **2005**, *44*, 2949.
[126] A. Brückner, J. Duparré, A. Bräuer, in *Proc. of SPIE – MOEMS and Miniaturized Systems VII*, (Eds: D. L. Dickensheets, H. Schenk), SPIE, San Jose, CA, USA **2008**, p. 688709.
[127] R. Horisaki, Y. Nakao, T. Toyoda, K. Kagawa, Y. Masaki, J. Tanida, *Opt. Rev.* **2009**, *16*, 241.
[128] A. Brückner, J. Duparré, P. Dannberg, A. Bräuer, A. Tünnermann, *Opt. Express* **2007**, *15*, 2109.
[129] J. Tanida, T. Kumagai, K. Yamada, S. Miyatake, K. Ishida, T. Morimoto, N. Kondou, D. Miyazaki, Y. Ichioka, *Appl. Opt.* **2001**, *40*, 1806.
[130] J. Duparr, P. Schreiber, P. Dannberg, T. Scharf, P. Pelli, R. Voelkel, H.-P. Herzig, A. Braeuer, in *Proc. of SPIE – MOEMS and Miniaturized Systems IV*, (Ed: A. El-Fatatry), SPIE, San Jose, CA, USA **2004**, p. 89.
[131] J. Duparré, P. Schreiber, A. Matthes, E. Pshenay-Severin, A. Bräuer, A. Tünnermann, R. VÖlkel, M. Eisner, T. Scharf, *Opt. Express* **2005**, *13*, 889.
[132] G. Druart, N. Guérineau, R. Haïdar, S. Thétas, J. Taboury, S. Rommeluère, J. Primot, M. Fendler, *Appl. Opt.* **2009**, *48*, 3368.
[133] M. K. Dobrzynski, R. Pericet-camara, D. Floreano, *IEEE Sens. J.* **2012**, *12*, 1131.
[134] W.-B. Lee, H. Jang, S. Park, Y. M. Song, H.-N. Lee, *Opt. Express* **2016**, *24*, 2013.
[135] J. L. Duncan, Y. Zhang, J. Gandhi, C. Nakanishi, M. Othman, K. E. H. Branham, A. Swaroop, A. Roorda, *Invest. Ophthalmol. Visual Sci.* **2007**, *48*, 3283.
[136] K. Zhang, L. Zhang, R. N. Weinreb, *Nat. Rev. Drug Discovery* **2012**, *11*, 541.
[137] E. Zrenner, *Science* **2002**, *295*, 1022.
[138] A. T. Chuang, C. E. Margo, P. B. Greenberg, *Br. J. Ophthalmol.* **2014**, *98*, 852.
[139] I. R. Minev, P. Musienko, A. Hirsch, Q. Barraud, N. Wenger, E. M. Moraud, J. Gandar, M. Capogrosso, T. Milekovic, L. Asboth, R. F. Torres, N. Vachicouras, Q. Liu, N. Pavlova, S. Duis, A. Larmagnac, J. Voros, S. Micera, Z. Suo, G. Courtine, S. P. Lacour, *Science* **2015**, *347*, 159.
[140] J. Park, S. Choi, A. H. Janardhan, S.-Y. Lee, S. Raut, J. Soares, K. Shin, S. Yang, C. Lee, K.-W. Kang, H. R. Cho, S. J. Kim, P. Seo, W. Hyun, S. Jung, H.-J. Lee, N. Lee, S. H. Choi, M. Sacks, N. Lu, M. E. Josephson, T. Hyeon, D.-H. Kim, H. J. Hwang, *Sci. Transl. Med.* **2016**, *8*, 344ra86.
[141] H. Lee, T. K. Choi, Y. B. Lee, H. R. Cho, R. Ghaffari, L. Wang, H. J. Choi, T. D. Chung, N. Lu, T. Hyeon, S. H. Choi, D.-H. Kim, *Nat. Nanotechnol.* **2016**, *11*, 566.
[142] G. Dagnelie, P. Christopher, A. Arditi, L. da Cruz, J. L. Duncan, A. C. Ho, L. C. O. de Koo, J.-A. Sahel, P. E. Stanga, G. Thumann, Y. Wang, M. Arsiero, J. D. Dorn, R. J. Greenberg, A. I. S. Grp, *Clin. Exp. Ophthalmol.* **2017**, *45*, 152.
[143] L. da Cruz, B. F. Coley, J. Dorn, F. Merlini, E. Filley, P. Christopher, F. K. Chen, V. Wuyyuru, J. Sahel, P. Stanga, M. Humayun, R. J. Greenberg, G. Dagnelie, A. I. S. Grp, *Brit. J. Ophthalmol.* **2013**, *97*, 632.
[144] E. Zrenner, K. U. Bartz-Schmidt, H. Benav, D. Besch, A. Bruckmann, V.-P. Gabel, F. Gekeler, U. Greppmaier, A. Harscher, S. Kibbel, J. Koch, A. Kusnyerik, T. Peters, K. Stingl, H. Sachs, A. Stett, P. Szurman, B. Wilhelm, R. Wilke, *Proc. R. Soc. B* **2011**, *278*, 1489.
[145] K. Stingl, K. U. Bartz-Schmidt, D. Besch, C. K. Chee, C. L. Cottriall, F. Gekeler, M. Groppe, T. L. Jackson, R. E. MacLaren, A. Koitschev, A. Kusnyerik, J. Neffendorf, J. Nemeth, M. A. N. Naeem, T. Peters, J. D. Ramsden, H. Sachs, A. Simpson, M. S. Singh, B. Wilhelm, D. Wong, E. Zrenner, *Vision Res.* **2015**, *111*, 149.
[146] J. D. Weiland, S. T. Walston, M. S. Humayun, *Annu. Rev. Vision Sci.* **2016**, *2*, 273.
[147] A. Ahnood, H. Meffin, D. J. Garrett, K. Fox, K. Ganesan, A. Stacey, N. V. Apollo, Y. T. Wong, S. G. Lichter, W. Kentler, O. Kavehei, U. Greferath, K. A. Vessey, M. R. Ibbotson, E. L. Fletcher, A. N. Burkitt, S. Prawer, *Adv. Biosyst.* **2017**, *1*, 1600003.
[148] J. D. Weiland, M. S. Humayun, H. Eckhardt, S. Ufer, L. Laude, B. Basinger, Y.-C. Tai, in *Annual Int. Conf. of the IEEE Engineering in Medicine and Biology Society*, IEEE, Minneapolis, MN, USA **2009**, p. 4140.
[149] I. L. Jones, M. Warner, J. D. Stevens, *Eye* **1992**, *6*, 556.
[150] P. Fattahi, G. Yang, G. Kim, M. R. Abidian, *Adv. Mater.* **2014**, *26*, 1846.
[151] S. Biswas, D. Sikdar, D. Das, M. Mahadevappa, S. Das, *Biomed. Microdevices* **2017**, *19*, 75.
[152] J. Jeong, S. H. Bae, K. S. Min, J.-M. Seo, H. Chung, S. J. Kim, *IEEE Trans. Biomed. Eng.* **2015**, *62*, 982.
[153] J. Kim, D. Son, M. Lee, C. Song, J.-K. Song, J. H. Koo, D. J. Lee, H. J. Shim, J. H. Kim, M. Lee, T. Hyeon, D.-H. Kim, *Sci. Adv.* **2016**, *2*, e1501101.
[154] S. J. Kim, K. W. Cho, H. R. Cho, L. Wang, S. Y. Park, S. E. Lee, T. Hyeon, N. Lu, S. H. Choi, D.-H. Kim, *Adv. Funct. Mater.* **2016**, *26*, 3207.
[155] L. Bareket, N. Waiskopf, D. Rand, G. Lubin, M. David-Pur, J. Ben-Dov, S. Roy, C. Eleftheriou, E. Sernagor, O. Cheshnovsky, U. Banin, Y. Hanein, *Nano Lett.* **2014**, *14*, 6685.
[156] C. G. Eleftheriou, J. B. Zimmermann, H. D. Kjeldsen, M. David-Pur, Y. Hanein, E. Sernagor, *Biomaterials* **2017**, *112*, 108.
[157] N. V. Apollo, M. I. Maturana, W. Tong, D. A. X. Nayagam, M. N. Shivdasani, J. Foroughi, G. G. Wallace, S. Prawer, M. R. Ibbotson, D. J. Garrett, *Adv. Funct. Mater.* **2015**, *25*, 3551.
[158] M. S. Humayun, J. D. Dorn, L. da Cruz, G. Dagnelie, J.-A. Sahel, P. E. Stanga, A. V. Cideciyan, J. L. Duncan, D. Eliott, E. Filley, A. C. Ho, A. Santos, A. B. Safran, A. Arditi, L. V. Del Priore, R. J. Greenberg, A. I. S. Grp, *Ophthalmology* **2012**, *119*, 779.
[159] W. Mokwa, M. Goertz, C. Koch, I. Krisch, H.-K. Trieu, P. Walter, in *Annual Int. Conf. of the IEEE Engineering in Medicine and Biology Society*, IEEE, Vancouver, BC, Canada **2008**, p. 5790.
[160] K. Mathieson, J. Loudin, G. Goetz, P. Huie, L. Wang, T. I. Kamins, L. Galambos, R. Smith, J. S. Harris, A. Sher, D. Palanker, *Nat. Photonics* **2012**, *6*, 391.
[161] D. Ghezzi, M. R. Antognazza, R. Maccarone, S. Bellani, E. Lanzarini, N. Martino, M. Mete, G. Pertile, S. Bisti, G. Lanzani, F. Benfenati, *Nat. Photonics* **2013**, *7*, 400.
[162] M. R. Antognazza, M. Di Paolo, D. Ghezzi, M. Mete, S. Di Marco, J. F. Maya-Vetencourt, R. Maccarone, A. Desii, F. Di Fonzo, M. Bramini, A. Russo, L. Laudato, I. Donelli, M. Cilli, G. Freddi, G. Pertile, G. Lanzani, S. Bisti, F. Benfenati, *Adv. Healthcare Mater.* **2016**, *5*, 2271.
[163] V. Gautam, D. Rand, Y. Hanein, K. S. Narayan, *Adv. Mater.* **2014**, *26*, 1751.
[164] N. W. Roberts, T.-H. Chiou, N. J. Marshall, T. W. Cronin, *Nat. Photonics* **2009**, *3*, 641.
[165] T. W. Cronin, R. L. Caldwell, J. Marshall, *Nature* **2001**, *411*, 547.